Table I. Effects of PEG-IFN-α2b and IFN-α2b on RCC cell proliferation in nude mice.

Treatment group	Number	Tumor weight (g, mean ± SE)	Body weight (g, mean ± SE on day 15)
Control (culture medium)	9	1.835±0.132	17.122±0.362
IFN-α2b (640 IU)	9	1.735±0.177	16.089±0.599
IFN-α2b (6,400 IU)	9	1.455±0.140	16.667±0.420
PEG-IFN-α2b (640 IU)	9	1.267±0.072[a,c]	16.156±0.308
PEG-IFN-α2b (6,400 IU)	9	1.160±0.075[b]	15.244±0.313
PEG-IFN-α2b (64,000 IU)	9	0.920±0.126[b]	16.922±0.601
PEG-IFN-α2b (640,000 IU)	8	0.444±0.077[b]	17.638±0.717

Cultured VMRC-RCW cells were subcutaneously transplanted in each nude mouse ($1.0x10^7$/mouse). Seven days later, when the largest diameter of the tumor reached ~10 mm, mice were treated twice per week with s.c. injection of PEG-IFN-α2b, IFN-α2b, or culture medium. All mice were sacrificed on day 15. [a]$p<0.01$ and [b]$p<0.001$ vs. control; [c]$p<0.05$ vs. the same concentration of IFN.

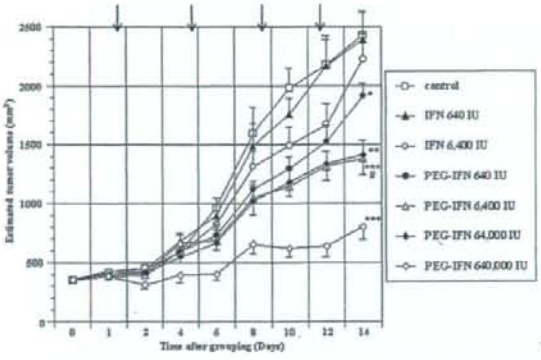

Figure 4. Chronological changes in the estimated volume of subcutaneously transplanted RCC tumors (VMRC-RCW cells, $1.0x10^7$) in nude mice according to the treatment dose. Seven days after the transplantation, when the largest tumor diameter reached ~10 mm (day 0), mice were divided into 7 groups (n=8 or 9, each). The arrows show the days of treatment. *p<0.05, **p<0.01 and ***p<0.001 vs. control; #p<0.01 vs. the same dose of IFN-α2b (6,400 IU). The values represent the average ± SE. PEG-IFN, PEG-IFN-α2b.

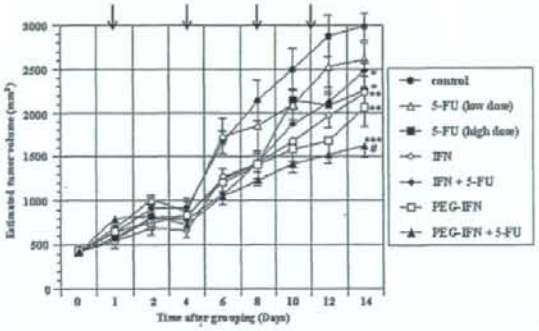

Figure 5. Chronological changes in the estimated volume of subcutaneously transplanted RCC tumors (VMRC-RCW cells, $7.5x10^6$) in nude mice according to the treatment method. Seven days after the transplantation, when the largest tumor diameter reached ~10 mm (day 0), mice were divided into 7 groups (n=8 or 9, each), i.e., PEG-IFN-α2b (6,400 IU) alone; IFN-α2b (6,400 IU) alone; combination of 5-FU and PEG-IFN-α2b (6,400 IU) or IFN-α2b (6,400 IU); 5-FU alone (low or high dose); and culture medium alone (control). The arrows show the days of treatment. *p<0.05, **p<0.01 and ***p<0.001 vs. control; #p<0.001 vs. IFN-α2b and 5-FU. The values represent the average ± SE. PEG-IFN, PEG-IFN-α2b.

Effects of the combination treatment of PEG-IFN-α2b and 5-FU on the growth of the VMRC-RCW cell line in vitro. Without 5-FU, the relative viable cell number did not decrease to 50% or lower of the control even when the highest dose of PEG-IFN-α2b (5,000 IU/ml) was added to the culture. When 5-FU (0.6 μM) was used in combination, the relative viable cell number was suppressed to 41.6% even when PEG-IFN-α2b was at the lowest dose (625 IU/ml, Fig. 2). The anti-proliferative effect of these two agents was additive, not synergistic.

Morphological examination in vitro. The 8 cell lines presented such apoptotic features as cytoplasmic shrinkage and chromatin condensation in a varying degree and in a dose-dependent manner at 72 h after adding PEG-IFN-α2b. For the combination treatment of PEG-IFN-α2b and 5-FU, more apoptotic cells were observed than in the PEG-IFN-α2b alone-treated cells, and the apoptotic cells increased dose-dependently to PEG-IFN-α2b plus 5-FU (Fig. 3).

Effects of PEG-IFN-α2b on RCC cell proliferation in nude mice. Chronological changes in estimated tumor volume after IFN administration to nude mice are summarized in Fig. 4. Dose-dependent suppression of tumor volume was observed in mice receiving PEG-IFN-α2b. The estimated tumor volume on day 14 in the mice receiving 6,400 IU of PEG-IFN-α2b became 61.9% of the mice receiving the same dose of IFN-α2b ($p<0.01$) and 56.8% of the control ($p<0.001$). The tumor weight on day 15 in the mice receiving 6,400 IU of PEG-IFN-α2b became 63.2% of the control ($p<0.001$, Table I).

Significant differences in the estimated tumor volume were observed between each PEG-IFN-α2b group (640, 6,400,

Table II. Effects of combination therapy of PEG-IFN-α2b and 5-FU on RCC cell proliferation in nude mice.

Treatment group	Number	Tumor weight (g, mean ± SE)	Body weight (g, mean ± SE on day 15)
Control (culture medium)	8	2.255±0.102	17.188±0.578
5-FU (low dose)	9	2.430±0.185	16.778±0.595
5-FU (high dose)	7	1.603±0.107[c]	15.686±0.814
IFN-α2b alone	8	1.812±0.084[b]	16.363±0.692
IFN-α2b + 5-FU	8	1.917±0.170	16.344±0.426
PEG-IFN-α2b	8	1.771±0.172[a]	15.963±0.459
PEG-IFN-α2b + 5-FU	9	1.742±0.194[a]	15.767±0.621

Cultured VMRC-RCW cells were subcutaneously transplanted in each nude mouse (7.5×10^6/mouse). Seven days later, when the largest diameter of the tumor reached ~10 mm, mice were treated with s.c. injection of IFNs and/or intraperitoneal injection of 5-fluorouracil (5-FU) daily. All mice were sacrificed on day 15. The concentration of both PEG-IFN-α2b and IFN-α2b was 6,400 IU/ml. [a]$p<0.05$, [b]$p<0.01$ and [c]$p<0.001$ vs. control.

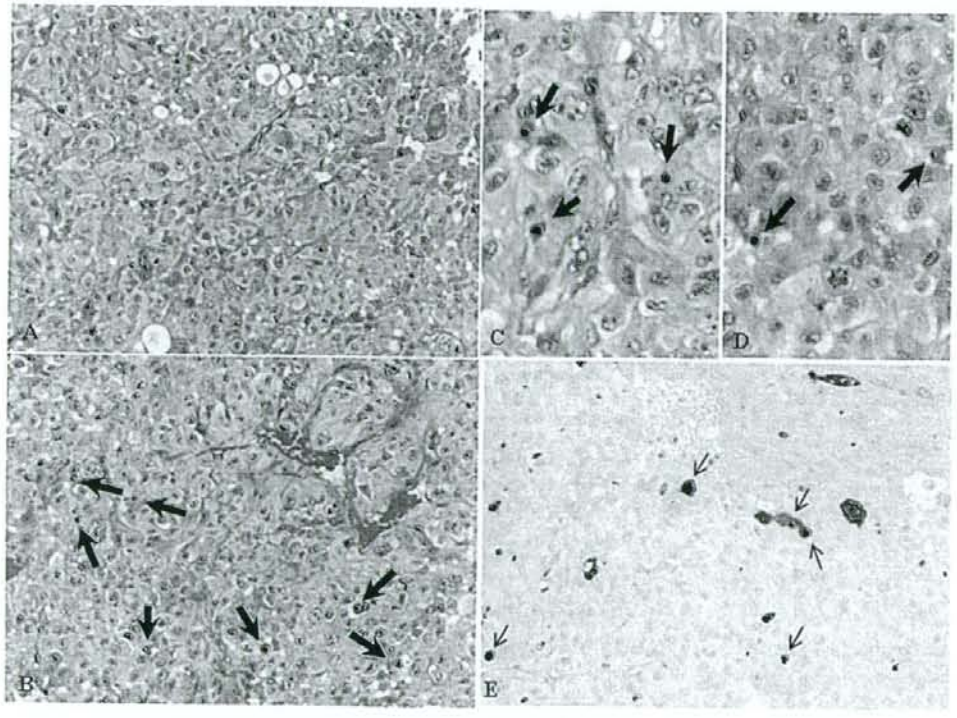

Figure 6. Photomicrograph of a subcutaneous human RCC tumor in nude mice, which developed after the injection of VMRC-RCW cells. (A) A control mouse that received culture medium alone. The tumor showed a thick trabecular arrangement of tumor cells and thin fibrous connective tissues and capillary vessels in the stroma. (B) A mouse that received PEG-IFN-α2b and 5-FU. There were many apoptotic tumor-cells (thick arrows, H&E staining, x200). (C and D) Higher magnifications of B (x400). Apoptotic tumor-cells characterized by shrinkage and eosinophilic change in the cytoplasm and chromatin condensation are shown (thick arrows, H&E staining). (E) TUNEL-positive apoptotic cells showing brown nuclei (thin arrows, TUNEL staining, x200).

64,000, 640,000 IU) and the control ($p<0.05$ to $p<0.001$, Fig. 3). There was no significant difference between 640 or 6,400 IU of the IFN-α2b group and the control. There were no significant differences in body weight of the mice among the groups.

Effects of the combination therapy of PEG-IFN-α2b and 5-FU on RCC cell proliferation in nude mice. Chronological changes in estimated tumor volume are shown in Fig. 5. The tumor volume on day 14 for the combination therapy of PEG-IFN-α2b and 5-FU was 54.2% of the control ($p<0.0001$).

Table III. Relative mRNA expression levels of the enzymes related with 5-FU metabolism, VEGF, VEGFR-1 and type I IFN receptor subunits.

Treatment group	DPD	TP	TK	TS	UP	OPRT	VEGF	VEGFR-1	IFNAR-1	IFNAR-2
5-FU (low dose)	129	101	68	182	59	48	116	135	122	94
5-FU (high dose)	72	50	52	40[a]	86	41	30	93	59	90
IFN-α2b	110	71	82	119	100	103	97	134	108	174
IFN-α2b + 5-FU	95	80	85	74	53	106	56	111	63	44[a,d]
PEG-IFN-α2b	648[b,d]	420[a]	313	297[b,d]	76	124	366[a,d]	277	159	217
PEG-IFN-α2b + 5-FU	159[c]	143[c]	162	129	129	86	251[a,e]	138	91	141

mRNA levels were examined by quantitative real-time RT-PCR and normalized with GAPDH. The values of relative mRNA expression level represent the average of the ratio to the level of control in each group. [a]p<0.05 and [b]p<0.01 vs. control; [c]p<0.05 vs. PEG-IFN-α2b; [d]p<0.05 vs. IFN-α2b; and [e]p<0.01 vs. IFN-α2b plus 5-FU. DPD, dihydropyrimidine dehydrogenase; TP, thymidine phosphorylase; TK, thymidine kinase; TS, thymidylate synthase; UP, uridine phosphorylase; OPRT, orotate phosphoribosyl transferase; VEGF, vascular endothelial growth factor; VEGFR-1, VEGF receptor 1; IFNAR-1, type I interferon receptor subunit 1; and IFNAR-2, type I interferon receptor subunit 2.

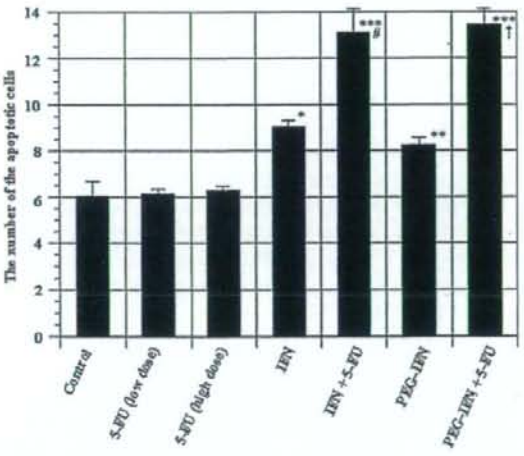

Figure 7. Number of apoptotic cells in the tumors. The number was counted in ten 0.25 mm² areas in each section, and the average number per area in each group was obtained. *p<0.05, **p<0.01 and ***p<0.001 vs. control; #p<0.05 vs. IFN-α2b; †p<0.001 vs PEG-IFN-α2b. PEG-IFN, PEG-IFN-α2b.

The tumor weights of the mice on day 15 were significantly different between the control and the 5-FU high dose group, each IFN alone group, and the combination group of PEG-IFN-α2b and 5-FU. The two types of IFNs and/or 5-FU did not affect the body weight of the mice (Table II).

Histological examination of the RCC tumor specimens stained with H&E revealed that the number of apoptotic cells was significantly higher in the mice treated with 6,400 IU of PEG-IFN-α2b (p<0.01) or 6,400 IU of IFN-α2b (p<0.05) in comparison to the control (Fig. 6A-D). The incidence of apoptosis in TUNEL-stained sections showed the same tendencies as those obtained in the H&E-stained sections (Fig. 6E). The number of apoptotic cells significantly increased in the mouse tumors treated with the combination therapy in comparison to the control (for each IFN, p<0.0001). The number also significantly increased with the combination treatment of PEG-IFN-α2b and 5-FU in comparison to PEG-IFN-α2b alone (p<0.0001), and with the combination of IFN-α2b and 5-FU in comparison to IFN-α2b alone (p<0.05, Fig. 7).

The results of quantitative real-time RT-PCR are shown in Table III. The VEGF mRNA levels increased significantly in the PEG-IFN-α2b alone group (p<0.05 vs. control, p<0.05 vs. IFN-α2b) and in the combination (PEG-IFN-α2b plus 5-FU) group (p<0.05 vs. control, p<0.01 vs. IFN-α2b plus 5-FU). There were also significant increases in the expression levels of DPD (p<0.01), TP (p<0.05), and TS (p<0.05) in the PEG-IFN-α2b alone group in comparison to the control. On the other hand, significant decreases were observed in the expression levels of DPD (p<0.05) and TP (p<0.05) in the combination (PEG-IFN-α2b plus 5-FU) group in comparison to the PEG-IFN-α2b alone group. In addition, the TS mRNA levels in the PEG-IFN-α2b group increased in comparison to the IFN-α2b group (p<0.05). The relative mRNA levels of IFN-α2b receptors in the combination group were lower than the levels of the IFN alone group.

The number of artery-like blood vessels increased slightly in comparison to the control in the groups receiving IFN-α2b alone, PEG-IFN-α2b alone, or the combination therapies; and there were no significant differences among the 7 groups (Fig. 8).

Discussion

Shang *et al* (18) examined 5 RCC cell lines and reported that the greatest decrease in the viable cell number after adding 1,600 IU/ml of Sumiferon to the cultures was 42% (58% of the control). On the other hand, Vyas *et al* (19) comparatively examined the anti-tumor effects of PEG-IFN-α2b and IFN-α2b by using an RCC cell line, ACHN, and reported that the addition of 1,033 IU/ml of PEG-IFN-α2b suppressed the viable cell number to 50% of the control. Our current

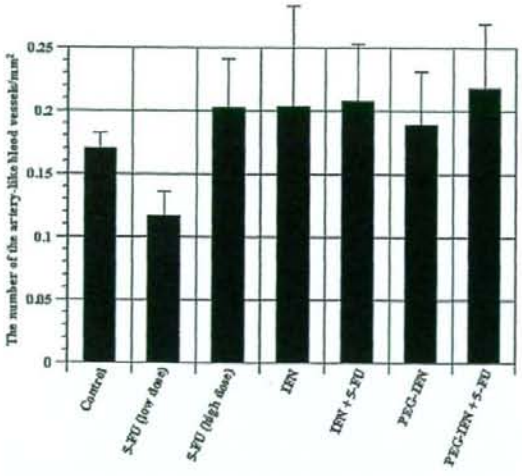

Figure 8. Number of artery-like blood vessels in the tumors. The number was counted in the whole area of each section, and mean number per mm² was obtained. Each figure shows the average ± SE. PEG-IFN: PEG-IFN-α2b.

experiment used concentration levels close to those of Shang *et al*, and similar anti-tumor effects were obtained. However, the level of suppression in our study did not reach 50% of the control even though the concentrations were higher than those of Vyas *et al*. The reasons for these disparate findings are not clear, however, they may be related to the different cell density in the experiments, different measurement methods, and possible changes in cell characteristics due to cultures. Vyas *et al* (19) also reported that the anti-tumor effects of PEG-IFN-α2b and IFN-α2b were not markedly different as we demonstrated in the present study.

Some medical institutions administer the combination therapy of IFN-α and 5-FU in the treatment for advanced RCC. Sella *et al* (20) reported that the combination of IFN-α and chemotherapy (5-FU and mitomycin C) resulted in a significant clinical effect on RCC patients. Our results support the anti-tumor effects reported by Sella *et al* regarding the combination of IFN-α and chemotherapy. Moreover, in the present study, the combination of PEG-IFN-α2b and 5-FU exhibited enhanced anti-tumor effects in comparison to the combination of IFN-α2b and 5-FU *in vivo*.

The induction of apoptosis is a mechanism of the anti-tumor effects of IFN-α2b, and Vyas *et al* (19) reported a dose-dependent increase in apoptotic cell number for PEG-IFN-α2b in cell cultures. Shang *et al* (18) found that apoptosis induction by IFN-α2b was not significant even at a dose of 5,000 IU/ml. On the other hand, 5-FU induced apoptosis in a dose-dependent manner, and 50 and 100 IU/ml of IFN-α2b was able to promote 5-FU-induced apoptosis in RCC cells. In our current study, the number of apoptotic cells *in vitro* increased proportionally to the dose of PEG-IFN-α2b and to the doses of PEG-IFN-α2b plus 5-FU in the combination treatment. The apoptotic cell number in the tumors also increased dose-dependently in the IFN-α2b alone group and PEG-IFN-α2b alone group, and the number in each group further increased with the combination of 5-FU. This indicates that PEG-IFN-α2b and IFN-α2b induced apoptosis and the combination with 5-FU induced apoptosis more extensively. Comparing the two combination treatments, i.e., PEG-IFN-α2b plus 5-FU vs. IFN-α2b plus 5-FU, the estimated tumor volume was significantly smaller in the PEG-IFN-α2b plus 5-FU group, but the number of apoptotic cells did not differ markedly between the groups. Shang *et al* (18) revealed that IFN-α2b caused cell cycle arrest at G1 in ACHN cells and at G2/M in Caki-1 cells in their flow cytometric analyses, and this suggests that cell cycle arrest could be the reason why there was no remarkable difference in the number of apoptotic cells in our results.

Anti-angiogenesis activity is a biological effect of IFN-α2b, and it has been shown that IFN-α2b inhibits angiogenesis by down-regulating angiogenesis factors. For example, Dinney *et al* (21) systematically administered IFN-α in a nude mouse model of bladder tumor and reported a decrease in *in vivo* blood vessel density in the tumors, which then resulted in the shrinkage of the tumor size. On the other hand, Kojiro *et al* (16) reported that there was no significant relation between the tumor shrinkage effects and angiogenesis factors or artery-like blood vessels when IFN-α and 5-FU were administered in combination to nude mice receiving transplantation of HCC cells. In our current study, the mRNA expression of VEGF and the number of artery-like blood vessels in the tumors were not suppressed in the PEG-IFN-α2b alone group and the PEG-IFN-α2b plus 5-FU group, but the estimated tumor volume of the PEG-IFN-α2b plus 5-FU group was the most suppressed among the groups. The reason for these contrary findings is unclear. Angiogenesis plays an important role in the proliferation and metastasis of solid tumors such as renal cancer, therefore the relation between angiogenesis factors and anti-tumor effects should be investigated in future studies by using different IFN preparations and other RCC cell lines.

It has been reported that IFN directly suppresses tumor proliferation and at the same time augments the suppressive effects of 5-FU on tumor growth, including the induction of apoptosis (15,22). In regards to the mechanism of this augmentation, several researchers reported that IFN-α acts on the metabolic pathway of 5-FU (23,24). Low levels of TS and DPD and high levels of OPRT, TP, UP and TK render cancer cells sensitive to 5-FU. In our results, the enzymes related to 5-FU metabolism, except OPRT, slightly increased (not significantly) in comparison to the control. Therefore, the activity of 5-FU-related enzymes were not related to the anti-tumor effects shown in our PEG-IFN-α2b plus 5-FU group.

IFN-α2b exerts its actions through a specific cell surface receptor, Type I IFN receptor, which consists of two subunits IFNAR-1 and IFNAR-2. IFNAR-2 is the binding subunit and is more important than IFNAR-1 for the expression of IFN-α2b activity (25-27). Oie *et al* (17) examined the expression of type I IFN receptor mRNA in 6 HCC cell lines treated with 5-FU. They showed that the expression of type I IFN receptor was markedly increased in the 3 cell lines whose proliferation was suppressed synergistically by the administration of 5-FU and IFN-α than in the other 3 cell lines whose proliferation was suppressed in an additive manner. In our current study, expression of IFNAR-1 and IFNAR-2 increased in the IFN-α2b alone and PEG-IFN-α2b alone groups, whereas the expression levels were markedly lower

in the combination groups of IFN-α plus 5-FU than in the IFN alone groups. These findings differ from those of Oie *et al* which could be the reason why the effects of our combination treatment were additive and not synergistic.

Our results confirmed that in the treatment of RCC, PEG-IFN-α2b presents more potent anti-tumor effects than conventional non-pegylated IFN-α2b, and the effects are augmented when 5-FU is used in combination. The most probable mechanism of this potent effect is apoptosis induction, and the target molecules that induce apoptosis will be determined in future studies. We expect that the addition of another agent to the combination of IFN-α2b and 5-FU would result in more potent anti-tumor effects in the treatment of RCC.

Acknowledgements

We thank Ms. Akemi Fujiyoshi for her assistance in our experiments. This study was supported by a Grant-in-Aid from the Ministry of Health, Labor and Welfare of Japan (no. 17200501) and by a Grant-in-Aid for Scientific Research (C) from the Ministry of Education, Science, Sports and Culture, Japan (no. 19590412).

References

1. Hartmann JT and Bokemeyer C: Chemotherapy for renal cell carcinoma. Anticancer Res 19: 1541-1543, 1999.
2. Atzpodien J, Lopez Hanninen E, Kirchner H, Bodenstein H, Pfreundschuh M, Rebmann U, Metzner B, Illiger HJ, Jakse G, Niesel T, *et al*: Multiinstitutional home-therapy trial of recombinant human interleukin-2 and interferon alfa-2 in progressive metastatic renal cell carcinoma. J Clin Oncol 13: 497-501, 1995.
3. Hernberg M, Pyrhonen S and Muhonen T: Regimens with or without interferon-alpha as treatment for metastatic melanoma and renal cell carcinoma: an overview of randomized trials. J Immunother 22: 145-154, 1999.
4. Dutcher JP, Logan T, Gordon M, Sosman J, Weiss G, Margolin K, Plasse T, Mier J, Lotze M, Clark J and Atkins M: Phase II trial of interleukin 2, interferon alpha, and 5-fluorouracil in metastatic renal cell cancer: a cytokine working group study. Clin Cancer Res 6: 3442-3450, 2000.
5. Wadler S and Wiernik PH: Partial reversal of doxorubicin resistance by forskolin and 1, 9-dideoxyforskolin in murine sarcoma S180 variants. Cancer Res 48: 539-543, 1988.
6. Baker DE: Pegylated interferon plus ribavirin for the treatment of chronic hepatitis C. Rev Gastroenterol Disord 3: 93-109, 2003.
7. Reddy KR, Wright TL, Pockros PJ, Shiffman M, Everson G, Reindollar R, Fried MW, Purdum PP III, Jensen D, Smith C, Lee WM, Boyer TD, Lin A, Pedder S and DePamphilis J: Efficacy and safety of pegylated (40-kd) interferon alpha-2a compared with interferon alpha-2a in noncirrhotic patients with chronic hepatitis C. Hepatology 33: 433-438, 2001.
8. Lindsay KL, Trepo C, Heintges T, Shiffman ML, Gordon SC, Hoefs JC, Schiff ER, Goodman ZD, Laughlin M, Yao R and Albrecht JK: A randomized, double-blind trial comparing pegylated interferon alfa-2b to interferon alfa-2b as initial treatment for chronic hepatitis C. Hepatology 34: 395-403, 2001.
9. Lee SD, Yu ML, Cheng PN, Lai MY, Chao YC, Hwang SJ, Chang WY, Chang TT, Hsieh TY, Liu CJ and Chen DS: Comparison of a 6-month course peginterferon alpha-2b plus ribavirin and interferon alpha-2b plus ribavirin in treating Chinese patients with chronic hepatitis C in Taiwan. J Viral Hepat 12: 283-291, 2005.
10. Bruno S, Camma C, Di Marco V, Rumi M, Vinci M, Camozzi M, Rebucci C, Di Bona D, Colombo M, Craxi A, Mondelli MU and Pinzello G: Peginterferon alfa-2b plus ribavirin for naive patients with genotype 1 chronic hepatitis C: a randomized controlled trial. J Hepatol 41: 474-481, 2004.
11. Yano H, Yanai Y, Momosaki S, Ogasawara S, Akiba J, Kojiro S, Moriya F, Fukahori S, Kurimoto M and Kojiro M: Growth inhibitory effects of interferon-alpha subtypes vary according to human liver cancer cell lines. J Gastroenterol Hepatol 21: 1720-1725, 2006.
12. Motzer RJ, Rakhit A, Ginsberg M, Rittweger K, Vuky J, Yu R, Fettner S and Hooftman L: Phase I trial of 40-kd branched pegylated interferon alfa-2a for patients with advanced renal cell carcinoma. J Clin Oncol 19: 1312-1319, 2001.
13. Yano H, Maruiwa M, Sugihara S, Kojiro M, Noda S and Eto K: Establishment and characterization of a new human renal cell carcinoma cell line (KRC/Y). In Vitro Cell Dev Biol 24: 9-16, 1988.
14. Hisaka T, Yano H, Ogasawara S, Momosaki S, Nishida N, Takemoto Y, Kojiro S, Katafuchi Y and Kojiro M: Interferon-alphaCon1 suppresses proliferation of liver cancer cell lines in vitro and in vivo. J Hepatol 41: 782-789, 2004.
15. Chou T-C and Talalay P: Analysis of combined drug effects: a new look at a very old problem. Trends Pharmacol Sci 4: 450-454, 1983.
16. Kojiro S, Yano H, Ogasawara S, Momosaki S, Takemoto Y, Nishida N and Kojiro M: Antiproliferative effects of 5-fluorouracil and interferon-alpha in combination on a hepatocellular carcinoma cell line in vitro and in vivo. J Gastroenterol Hepatol 21: 129-137, 2006.
17. Oie S, Ono M, Yano H, Maruyama Y, Terada T, Yamada Y, Ueno T, Kojiro M, Hirano K and Kuwano M: The up-regulation of type I interferon receptor gene plays a key role in hepatocellular carcinoma cells in the synergistic antiproliferative effect by 5-fluorouracil and interferon-α. Int J Oncol 29: 1469-1478, 2006.
18. Shang D, Ito N, Watanabe J, Awakura Y, Nishiyama H, Kamoto T and Ogawa O: Synergy of interferon-alpha and 5-fluorouracil in human renal cell carcinoma requires p53 activity. Eur Urol 52: 1131-1139, 2007.
19. Vyas K, Brassard DL, DeLorenzo MM, Sun Y, Grace MJ, Borden EC and Leaman DW: Biologic activity of polyethylene glycol 12000-interferon-alpha2b compared with interferon-alpha2b: gene modulatory and antigrowth effects in tumor cells. J Immunother 26: 202-211, 2003.
20. Sella A, Logothetis CJ, Fitz K, Dexeus FH, Amato R, Kilbourn R and Wallace S: Phase II study of interferon-alpha and chemotherapy (5-fluorouracil-and mitomycin C) in metastatic renal cell cancer. J Urol 147: 573-577, 1992.
21. Dinney CP, Bielenberg DR, Perrotte P, Reich R, Eve BY, Bucana CD and Fidler IJ: Inhibition of basic fibroblast growth factor expression, angiogenesis, and growth of human bladder carcinoma in mice by systemic interferon-alpha administration. Cancer Res 58: 808-814, 1998.
22. Oka Y, Naomoto Y, Yasuoka Y, Hatano H, Haisa M, Tanaka N and Orita K: Apoptosis in cultured human colon cancer cells induced by combined treatments with 5-fluorouracil, tumor necrosis factor-alpha and interferon-alpha. Jpn J Clin Oncol 27: 231-235, 1997.
23. Kase S, Kubota T, Watanabe M, Teramoto T, Kitajima M and Hoffman RM: Recombinant human interferon alpha-2a increases 5-fluorouracil efficacy by elevating fluorouridine concentration in tumor tissue. Anticancer Res 14: 1155-1159, 1994.
24. Schwartz EL, Hoffman M, O'Connor CJ and Wadler S: Stimulation of 5-fluorouracil metabolic activation by interferon-alpha in human colon carcinoma cells. Biochem Biophys Res Commun 182: 1232-1239, 1992.
25. Pestka S, Langer JA, Zoon KC and Samuel CE: Interferons and their actions. Annu Rev Biochem 56: 727-777, 1987.
26. Lutfalla G, Holland SJ, Cinato E, Monneron D, Reboul J, Rogers NC, Smith JM, Stark GR, Gardiner K, Mogensen KE, *et al*: Mutant U5A cells are complemented by an interferon-alpha beta receptor subunit generated by alternative processing of a new member of a cytokine receptor gene cluster. EMBO J 14: 5100-5108, 1995.
27. Domanski P, Witte M, Kellum M, Rubinstein M, Hackett R, Pitha P and Colamonici OR: Cloning and expression of a long form of the beta subunit of the interferon alpha beta receptor that is required for signaling. J Biol Chem 270: 21606-21611, 1995.

Biochemical and Biophysical Research Communications 377 (2008) 826–831

Contents lists available at ScienceDirect

Biochemical and Biophysical Research Communications

journal homepage: www.elsevier.com/locate/ybbrc

Role of macrophages in inflammatory lymphangiogenesis: Enhanced production of vascular endothelial growth factor C and D through NF-κB activation ☆

Kosuke Watari [a,b], Shintaro Nakao [a], Abbas Fotovati [a], Yuji Basaki [a], Fumihito Hosoi [a], Biborka Bereczky [a], Ryuichi Higuchi [b], Tomofumi Miyamoto [b], Michihiko Kuwano [c], Mayumi Ono [a,*]

[a] Department of Pharmaceutical Oncology, Graduate School of Pharmaceutical Sciences, Kyushu University, Maidashi 3-1-1, Higashi-ku, Fukuoka 812-8582, Japan
[b] Department of Natural Products Chemistry, Graduate School of Pharmaceutical Sciences, Kyushu University, Fukuoka 812-8582, Japan
[c] Innovation Center for Medical Redox Navigation, Kyushu University, Fukuoka 812-8582, Japan

ARTICLE INFO

Article history:
Received 26 September 2008
Available online 23 October 2008

Keywords:
IL-1β
Lymphangiogenesis
Inflammation
VEGF-C
VEGF- D
VEGFR-3
Macrophage

ABSTRACT

The close association of inflammation, angiogenesis and cancer progression is now highlighted, and in this study we especially focused on a close association of inflammation and lymphangiogenesis. We found that proinflammatory cytokine, interleukin-1β (IL-1β), could induce lymphangiogenesis in mouse cornea through enhanced production of potent lymphangiogenic factors, VEGF-A, VEGF-C and VEGF-D. IL-1β-induced lymphangiogenesis, but not angiogenesis, was inhibited by administration of a selective anti-VEGF receptor-3 (VEGFR-3) neutralizing antibody. And in mouse cornea we observed recruitment of monocyte/macrophages and neutrophils by IL-1β implanted cornea. Depletion of macrophages by a bisphosphonate encapsulated in liposomes inhibited this IL-1β-induced lymphangiogenesis and also up-regulation of VEGF-A, VEGF-C, and VEGF-D. Furthermore, IL-1β-induced lymphangiogenesis and angiogenesis were suppressed by NF-κB inhibition with marked suppression of VEGF-A, VEGF-C, and VEGF-D expression.

Recently great progress has been made in understanding the mechanisms of lymphangiogenesis as a direct result of the discovery of a number of specific factors with essential roles in embryonic and postnatal lymphangiogenesis as well as pathological lymphangiogenesis. These lymphangiogenesis-related factors include prospero-related homeobox 1 (Prox-1), vascular endothelial growth factor C (VEGF-C), VEGF-D, vascular endothelial growth factor receptor-3 (VEGFR-3), lymphatic vessel endothelial hyaluronan receptor 1 (LYVE-1), podoplanin [1] and others. Of these, VEGF-C and VEGF-D are known to act as potent lymphangiogenesis factors by binding to their receptors, VEGFR-2 and VEGFR-3, both of which are expressed on LECs. Two other growth factors, VEGF-A and FGF-2, which are known to be potent angiogenic factors, also promote lymphangiogenesis [2,3]. FGF-2 has been shown to induce lymphangiogenesis in the mouse cornea via two pathways: first, by direct interaction with its cognate receptors on LECs; and second, by indirect activation of VEGF-C/VEGFR-3 signaling [4,5]. The development of novel lymphatic vessels is therefore regulated both by some factors that are common to angiogenesis, and by some factors that are specific for lymphangiogenesis.

The lymphatic vasculature plays an important role in the pathogenesis of human diseases such as cancer, lymphadenoma, and inflammatory disorders [1]. In particular, the development of novel lymphatic vessels is dependent upon Prox-1, VEGF-C, and VEGF-D expression and is closely associated with tumor metastasis [6]. Proinflammatory cytokines often enhance the expression of VEGF-C [7] as well as VEGF-A [8,9] during inflammation, and constitutively activate the transcription factor which typifies inflammation, nuclear factor-κB (NF-κB) [10]. Cursiefen et al. reported that VEGF-A-mediated lymphangiogenesis in inflamed corneas could be attributable to the recruitment of macrophages which produce VEGF-C and VEGF-D [2]. A study by Hamrah et al. showed that the expression of VEGF-C and its receptor VEGFR-3 is up-regulated in corneal dendritic cells after cauterization of the corneal surface in mice [11]. In mouse models of chronic respiratory tract inflammation, the growth of lymphatic vessels was found to be dependent upon VEGFR-3 signaling, but the growth of blood vessels was not [12]. In addition, dendritic cells, macrophages, neutrophils, and epithelial cells in the respiratory tract have been shown to express the VEGFR-3 ligands, VEGF-C and VEGF-D, which evoke lymphangiogenesis without hemangiogenesis [12]. These studies strongly suggest a relationship between

☆ *Acknowledgment of research support:* This research was supported by a grant-in-aid for Scientific Research for Priority areas, Cancer, from the Ministry of Education Culture, Sports, Science and Technology of Japan (M.O.), and by the 3rd Term Comprehensive Control Research for Cancer from the Ministry of Health, Labor and Welfare, Japan (M.K.). This study was also supported in part by the Formation of Innovation Center for Fusion of Advanced Technologies, Kyushu University, Japan (M.O., M.K.).

* Corresponding author. Fax: +81 92 642 6296.
E-mail address: mono@phar.kyushu-u.ac.jp (M. Ono).

0006-291X/$ - see front matter © 2008 Elsevier Inc. All rights reserved.
doi:10.1016/j.bbrc.2008.10.077

lymphangiogenesis and the recruitment of leucocytes such as monocytes/macrophages and dendritic cells of monocytic lineage, to the cornea and other tissues undergoing inflammation.

Interleukin-1β (IL-1β) is a proinflammatory cytokine, and is the prototypical multifunctional cytokine that affects most cell types, often in accordance with other cytokines and low-molecular weight mediators [13]. IL-1β is present in the circulation of patients with a variety of diseases that involve infectious or inflammatory responses [14]. IL-1β and related inflammatory mediators enhance the expression of potent angiogenic factors such as interleukin-8 (IL-8) and VEGF-A resulting in the promotion of angiogenesis by both autocrine and paracrine mechanisms [8,9,15]. We previously reported that IL-1β could induce angiogenesis by enhancing the expression of prostanoids, CXC chemokines including IL-8, and VEGF-A, in the mouse cornea and in the tumor xenograft model of experimental angiogenesis [16,17]. Nakao and colleagues [18] have demonstrated that IL-1β-induced angiogenesis in mouse corneas is blocked by dexamethasone through its attenuation of NF-κB activating signaling. Ristimaki et al. have reported that IL-1β can also increase the expression of VEGF-C in human lung fibroblasts [7]. Although inflammation induced by corneal injury stimulates lymphangiogenesis [2,11,19], it remains unclear whether IL-1β itself can induce lymphangiogenesis.

In the present study, we examined the mechanism underlying the inflammatory cytokine IL-1β-induced lymphangiogenesis in mouse cornea. In addition, we considered the possible involvement of activated monocytes and macrophages in lymphangiogenesis in the response to inflammatory stimuli in corneas.

Materials and methods

Animals. All of the animal experiments were approved by the Committee on the Ethics of Animal Experiments at the Kyushu University, Japan. The male C57Bl/6 mice, aged 6–10 weeks, were purchased from Kyudo (Saga, Japan).

Cells and reagents. Recombinant human IL-1β and FGF-2 were purchased from R&D Systems (Minneapolis, MN). Phosphatidylcholine, cholesterol, clodronate, and anti-α-SMA were purchased from Sigma-Aldrich (St Louis, MO). The NF-κB inhibitor SN50 was purchased from Biomol International (Plymouth Meeting, PA). Lymphatic endothelial cells (LECs) were purchased from Lonza Biologics Inc. (Portsmouth, NH) and cultured according to

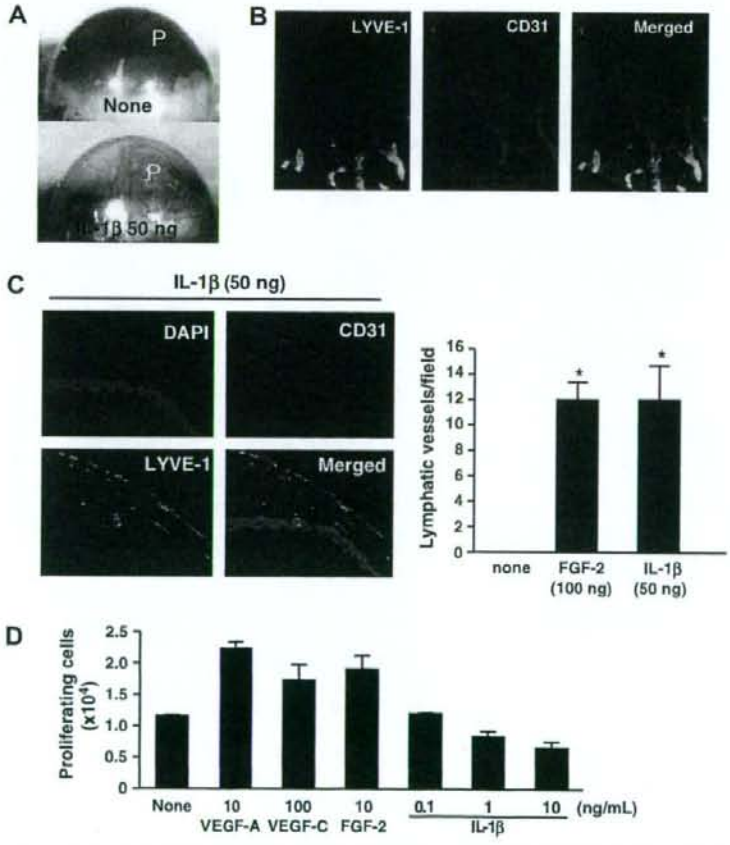

Fig. 1. Effect of IL-1β on corneal angiogenesis and lymphangiogenesis in mice. (A) Corneal neovascularization stimulated by implanted Hydron pellets (P) with or without 50 ng IL-1β was photographed 14 day later, in the region around the implants. (B) Whole corneal mount immunostained for LYVE-1 (green) and CD31 (red). (C) Immunostaining of LYVE-1 (green), CD31 (red), and DAPI (blue) in corneas treated with 50 ng IL-1β for 14 days. Quantification of lymphatic vessels in the corneas of mice treated with IL-1β and FGF-2. The number of lymphatic vessels was determined by scoring LYVE-1$^+$ vessels. The data represent the means ± SD. *Significant difference ($P<0.01$). (D) Effect of VEGF-A, VEGF-C, VEGF-D, FGF-2, or IL-1β on LEC proliferation. The data represent the means ± SDs of triplicate dishes.

the manufacture's instructions. Anti-podoplanin was purchased from Angiobio (Del Mar, CA). PE-conjugated anti-mouse CD31 (PECAM-1) Ab was from BD Bioscience (San Jose, CA). Anti-F4/80 was from Serotec (Atlanta, GA). Anti-Gr-1 Ab was from Cayman Chemical Co. (Ann Arbor, MI).

Proliferation assay by LEC. The LECs were suspended in Eagle's basal medium 2 supplemented with 2% fetal bovine serum (FBS) and growth factors. After 2.5×10^4 cells were seeded in 24-well plates (IWAKI, Tokyo, Japan) and incubated for 24 h at 37 °C, the medium was changed to Eagle's basal medium 2 containing 0.5% FBS with VEGF-A, VEGF-C, FGF-2, or IL-1β in each well. After 48 h incubation, cell number in each well was counted.

Corneal micropocket assay in mice. A corneal micropocket assay was used to quantify corneal neovascularization in response to 0.3 μL Hydron pellets (IFN Sciences, NJ) containing 50 ng human IL-1β or human FGF-2, together with 500 ng rat anti-mouse VEGFR-3 antibody [20] in some cases, which were implanted in the corneas of the mice. The pellets were positioned 1 mm away from the corneal limbus. After 14 days, the corneal vessels were photographed and recorded using Viewfinder 3.0 (Pixera) with standardized illumination and contrast, and were then saved to disk. Liposome-encapsulated clodronate (Cl_2MDP-LIPs) was prepared as described previously [17]. Cl_2MDP-LIPs (200 μL) were injected intravenously and 10 μL Cl_2MDP-LIPs were injected subconjunctivally every other day. As a control, the same doses of PBS-LIPs were administered through the dual routs every other day. On the other hand, to examine the effect of a NF-κB inhibition using of NF-κB inhibitor, SN50 (25 μg/μL, 3 μL eye drops) were applied topically to IL-1β implanted eyes twice a day from day −1 to day 13. The quantitative analysis of neovascularization in the mouse corneas was performed using the National Institutes of Health image software package. Immunohistochemical staining and quantitative real-time PCR were performed as described previously [17].

Double-labeling whole mounts for LYVE-1 and CD31. The mouse eyes were enucleated on day 6 or 14 after implanting pellets containing IL-1β or FGF-2. The corneal tissue was dissected, fixed in cold 4% PFA for 1 h, and digested with 20 μg/mL proteinase K at 4 °C for overnight. The whole mounts were immunostained with a mixture of anti- LYVE-1 polyclonal Ab [21] and anti-CD31, followed by biotinylated anti-rabbit IgG (Vector Laboratories), as a secondary Ab, overnight at 4 °C. The Blood and lymphatic vessels were examined, and photographed under a Zeiss confocal microscope.

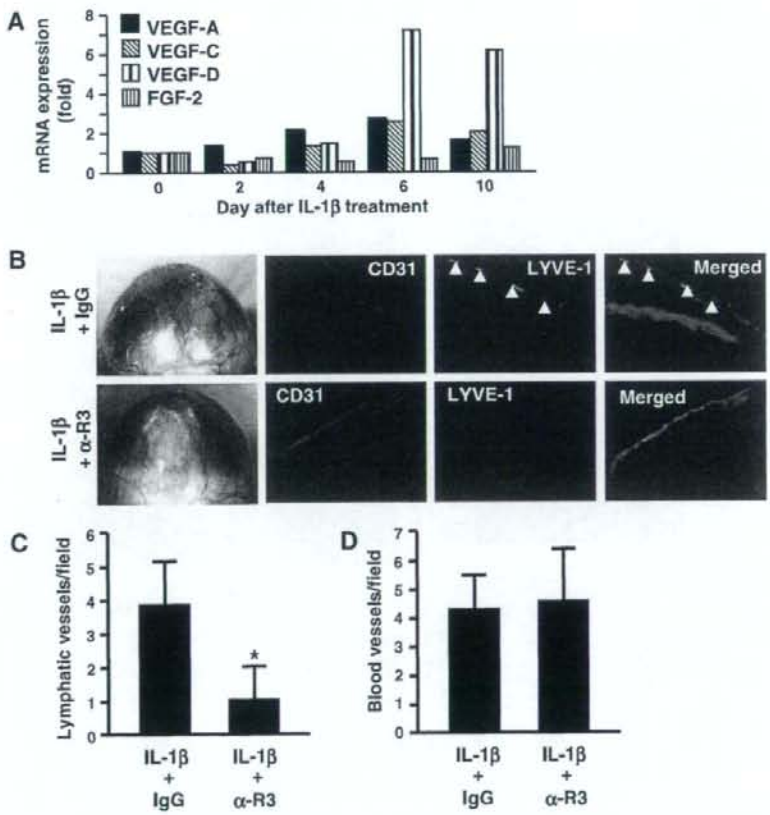

Fig. 2. Expression of VEGF family proteins and effect of neutralizing VEGFR-3 Ab on IL-1β-induced lymphangiogenesis. (A) Expression of VEGF-A, VEGF-C, VEGF-D, and FGF-2 in IL-1β-treated mouse corneas. The results shown were normalized to GAPDH mRNA levels and to corneal mRNA levels for each factor on day 0 (untreated control). Each value is the mean of six mice, and each mRNA level was within 5% of the mean value. (B) Hydron pellets containing 50 ng IL-1β with anti-VEGFR-3 Ab or control IgG Ab was implanted into the corneas of mice. After 14 days, frozen section of vessels were immunostained for LYVE-1 (green), CD31 (red), and DAPI (blue). (C) Quantification of lymphatic vessels and blood vessels by scoring LYVE-1$^+$ and CD31$^+$ vessels, respectively. All results are the means with the SDs ($n = 5$). *Significant difference ($P < 0.05$).

Results and discussion

IL-1β induces lymphangiogenesis as well as angiogenesis in mouse corneas, and the effect of VEGF-A, VEGF-C, FGF-2, and IL-1β on cell proliferation by LECs

In this study, we examined whether IL-1β could also induce lymphangiogenesis. The implantation of pellets containing 50 ng IL-1β induced neovascularization in the corneas of mice (Fig. 1A). Immunostaining whole mounts revealed the development of both LYVE-1$^+$ lymphatic vessels and CD31$^+$ blood vessels on day 14 after the implantation of pellets containing 50 ng IL-1β (Fig. 1B). Immunostaining of the corneal sections revealed the formation of both new lymphatic vessels and blood vessels (Fig. 1C). Quantification of the extent of lymphangiogenesis showed that 50 ng IL-1β induced new lymphatic vessels, and these numbers were comparable to those induced by 100 ng FGF-2 (Fig. 1C). By contrast, 10 ng IL-1β or 200 ng VEGF-A induced much less lymphatic vessels in the cornea (data not shown). These LYVE-1$^+$ vessels did not contain blood cells and did not express α-SMA, and most of these LYVE-1$^+$ vessels were also found to be positive for podoplanin, another lymphatic vessel specific marker (data not shown). We also observed LYVE-1$^+$ vessels in FGF-2-implanted corneas (Fig. 1C). We next examined whether IL-1β could directly stimulate angiogenic activity by looking its effects on proliferation and migration of LECs *in vitro*. LEC proliferation in culture was increased in response to exogenous VEGF-A, VEGF-C, and FGF-2, but was not affected by various doses of IL-1β (Fig. 1D). IL-1β at dose of 1 ng/mL was found to inhibit LEC proliferation (Fig. 1D), and IL-1β did not stimulate cell migration (data not shown).

Increased expression of VEGF family proteins in IL-1β-treated mouse corneas and inhibition of IL-1β-induced lymphangiogenesis by anti-VEGFR-3 antibody

We next examined the effect of IL-1β on the expression of the lymphangiogenesis-related factors VEGF-C, VEGF-D, and FGF-2, and the potent angiogenic factor, VEGF-A, in mouse cornea on day 0, 2, 4, 6, and 10. The VEGF-A, VEGF-C, and VEGF-D mRNA levels were increased with the time after IL-1β implantation in mice (Fig. 2A). The VEGF-A mRNA levels were markedly elevated on day 4 and followed a marked increase of VEGF-C and VEGF-D mRNA levels on day 6 and 10. VEGF-C and VEGF-D mediate their potent lymphangiogenic effects through their receptor, VEGFR-3, and neutralizing

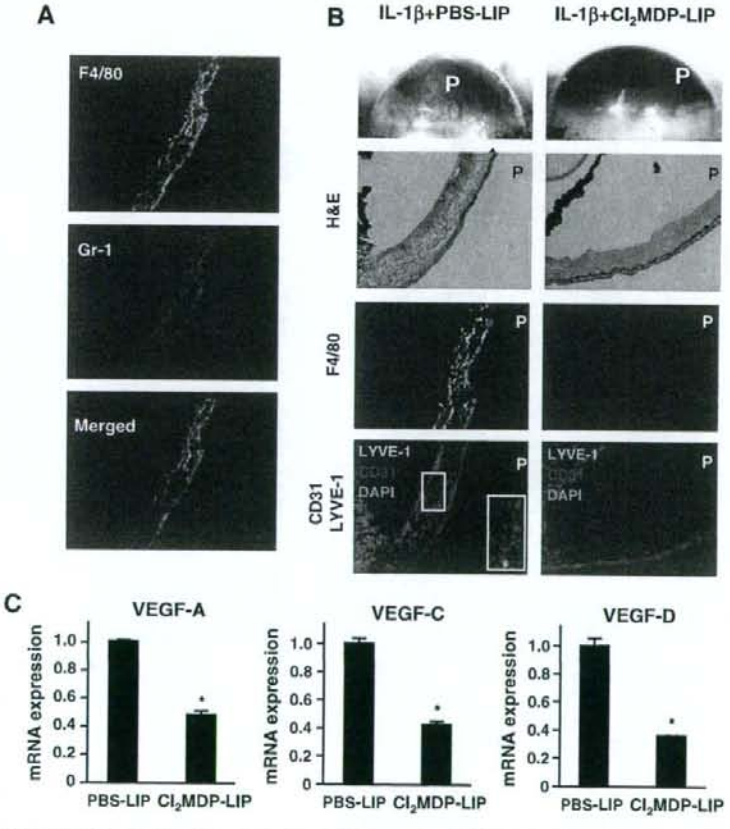

Fig. 3. Effect of macrophage depletion on IL-1β-induced lymphangiogenesis and mRNA expression of VEGF-A, VEGF-C, and VEGF-D. (A) Hydron pellets with or without 50 ng IL-1β were implanted into the corneas, and after 14 days, corneas were immunostained for monocyte/macrophages (F4/80, green), and neutrophils (Gr-1, red). (B) Hydron pellets (P) containing 50 ng IL-1β were implanted into the corneas of mice with or without administration of Cl_2MDP-LIP. After 14 days, vessels in the region of the pellet implants were immunostained for LYVE-1 (green), CD31 (red), DAPI (blue), and F4/80 (green). (C) Expression of VEGF-A, VEGF-C, and VEGF-D mRNAs in control and Cl_2MDP-LIP-treated corneas. Expression of VEGF family mRNAs was determined by quantitative RT-PCR. *Significant difference ($P<0.01$).

anti-VEGFR-3 Ab has been shown to selectively inhibit VEGF-C-induced lymphangiogenesis [22,23]. Treatment with anti-VEGFR-3 Ab (α-R3) had no apparent effect on IL-1β-induced angiogenesis, but inhibited the IL-1β-induced formation of LYVE-1$^+$ lymphatic vessels (Fig. 2B). Quantitative analysis demonstrated a significant ($P<0.05$) reduction in IL-1β-induced lymphangiogenesis by the α-R3 Ab (Fig. 2C). By contrast, α-R3 Ab did not affect the IL-1β-induced formation of CD31$^+$ vascular endothelial cells.

Effect of macrophage depletion on IL-1β-induced lymphangiogenesis and production of lymphangiogenic factors in vivo

Immunohistochemical analysis with the neutrophil-specific anti-Gr-1Ab and the macrophage-specific anti-F4/80 Ab revealed the infiltration of these inflammatory cells in IL-1β-induced lymphatic vessels and blood vessels in the cornea (Fig. 3A). We previously reported that IL-1β-induced angiogenesis in the mouse cornea was markedly suppressed when the macrophages in corneas and blood were depleted to 10–20% of the normal number by administration of Cl_2MDP-LIP via intravenous and subconjunctive injections [17]. Administration of Cl_2MDP-LIP markedly reduced the number of F4/80$^+$ macrophages in the cornea and also markedly inhibited angiogenesis (CD31$^+$ cells) and lymphangiogenesis (LYVE-1$^+$ cells) induced by IL-1β (Fig. 3B). Quantitative analysis demonstrated that mRNA levels of VEGF-A, VEGF-C, and VEGF-D in cornea were reduced by 50% or more in IL-1β-implanted mice only when the macrophages was depleted by Cl_2MDP-LIP (Fig. 3C). Taken together, macrophage depletion also affected the expression of VEGF-C, VEGF-D, and VEGF-A mRNA expression as well as lymphangiogenesis in IL-1β-treated corneas.

Effect of NF-κB inhibition on IL-1β-induced lymphangiogenesis and production of lymphangiogenic factors in vivo

To examine the role of NF-κB in the IL-1β-induced lymphangiogenesis and angiogenesis in the mouse corneas, we examined the effect of selective NF-κB inhibitor peptide, SN50. Typical examples of immunostaining whole mounts showed both LYVE-1$^+$ lymphatic vessels and CD31$^+$ blood vessels on day 14 after IL-1β implantation with or without SN50 (Fig. 4A). Quantitative analysis resulted in significant reduction of both angiogenesis and lymphangiogenesis by SN50 treatment in comparison with the untreated control group (Fig. 4B). Expression of VEGF-C and VEGF-D was markedly reduced to 20% or less in IL-1β-treated mice by SN50 as compared with control mice when those of VEGF-A mRNAs were reduced to about 50% (Fig. 4C). NF-κB activation thus might play a key role in the inflammatory cytokine-induced lymphangiogenesis and production of potent lymphangiogenic factors.

The activation of VEGFR-3 by its cognate ligands such as VEGF-C and VEGF-D has been reported to induce proliferation and migration by LEC [22]. Our *in vitro* study indicated that VEGF-A, VEGF-C, and FGF-2 stimulated proliferation and migration by LEC, but that IL-1β itself had no stimulatory effect on proliferation and

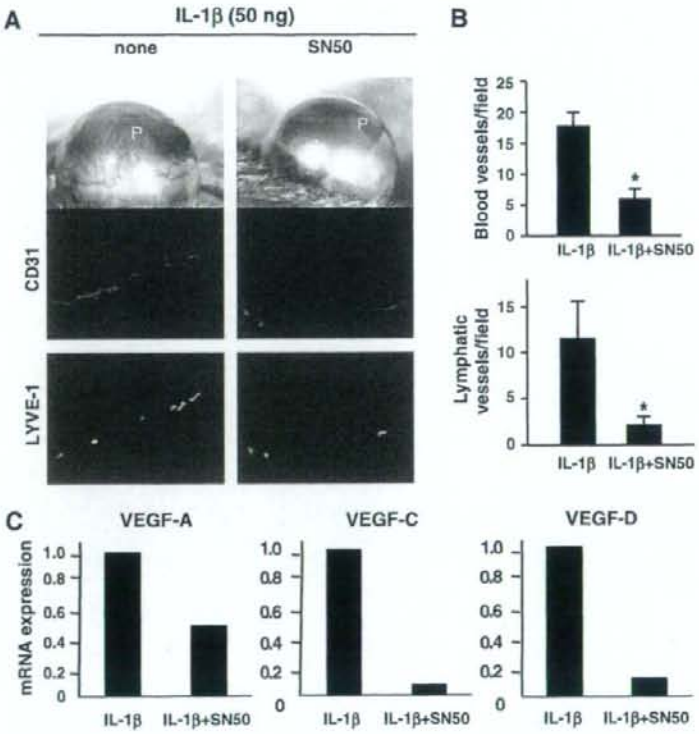

Fig. 4. Effect of NF-κB inhibition on IL-1β-induced corneal neovascularization and neolymphangiogenesis. (A) IL-1β-implanted corneas were topically treated with or without SN50. Immunostaining of CD31 (red) and LYVE-1 (green) in corneas treated with 50 ng IL-1β for 14 days with or without SN50. (P: pellet) (B) Quantification of blood vessels and lymphatic vessels in the corneas of mice treated with IL-1β in the absence or presence of SN50 for 14 days ($n=6$). (C) Expression of VEGF-A, VEGF-C, and VEGF-D mRNAs in untreated control and SN50-treated corneas. Expression of VEGF family mRNAs was determined by quantitative RT-PCR. *Significant difference ($P<0.05$).

migration. Furthermore, IL-1β-induced lymphangiogenesis was inhibited by simultaneous treatment with anti-VEGFR-3 Ab. IL-1β stimulated the expression of VEGF-A, VEGF-C, and VEGF-D, but not FGF-2, in cornea. As the interaction of VEGF-C and VEGF-D with VEGFR-3 selectively activates pro-lymphangiogenic signaling [1,6], IL-1β-induced lymphangiogenesis appears to be attributable to an indirect paracrine mechanism acting through VEGF-C/VEGF-D/VEGFR-3 signaling, rather than by a direct interaction with the IL-1β receptor.

IL-1β-induced inflammatory angiogenesis in mouse corneas was markedly blocked by a potent anti-inflammatory drug dexamethasone [18]. Dexamethasone inhibited NF-κB activation in corneal stromal cells, and treatment with a NF-κB inhibitory peptide SN50 markedly blocked the IL-1β-induced angiogenesis, suggesting NF-κB activating signaling was at least in part involved in the inflammatory cytokine-induced angiogenesis in corneas [18]. Consistent with this study, topical administration of SN50 blocked IL-1β-induced angiogenesis in corneas. Furthermore, administration of SN50 resulted in marked inhibition of both IL-1β-induced lymphangiogenesis and production of VEGF-C, VEGF-D, and VEGF-A (Fig. 4). Treatment of macrophages with IL-1β *in vitro* also enhanced production of VEGF-A and VEGF-D, and that this IL-1β-induced production of VEGF-A was blocked by a NF-κB inhibitor *in vitro* [24]. IL-1β-induced lymphangiogenesis as well as angiogenesis thus might be in part mediated by VEGF family proteins through activation of NF-κB, and favorably through NF-κB activated macrophages in corneal stroma.

In our present study, we have presented evidence that IL-1β can induce lymphangiogenesis in the mouse cornea, and that this activity is mediated by the up-regulation of potent lymphangiogenic factors VEGF-C, VEGF-D, and VEGF-A, together with recruitment and activation of macrophages in response to the inflammatory stimuli. IL-1β also induces angiogenesis in both corneas and tumors in mice, dependent on infiltrating macrophages through enhanced production of VEGF family proteins, IL-8 and matrix metalloproteases [13]. Taken together, the inflammatory cytokine IL-1β could induce not only angiogenesis but also lymphangiogenesis, supporting the idea of close link between inflammation and lymphangiogenesis as well as angiogenesis [13]. Macrophages play a key role in the IL-1β-induced lymphangiogenesis, and both macrophages and NF-κB pathway could be potent targets to develop drugs to control the inflammatory lymphangiogenesis in cancer.

Acknowledgments

We thank S. Nishikawa (Kyoto University) for supplying us rat anti-mouse VEGFR-3 antibody. We also thank K. Nakagawa, T. Nakano, and K. Sueishi (Kyushu University) for fruitful discussion.

References

[1] K. Alitaro, T. Tammela, T.V. Petrova, Lymphangiogenesis in development and human disease, Nature 438 (2005) 946–953.
[2] C. Cursiefen, L. Chen, L.P. Borges, D. Jackson, J. Cao, C. Radziejewski, P.A. D'Amore, M.R. Dana, S.J. Wiegand, J.W. Streilein, VEGF-A stimulates lymphangiogenesis and hemangiogenesis in inflammatory neovascularization via macrophage recruitment, J. Clin. Invest. 113 (2004) 1040–1050.
[3] S. Hirakawa, M. Detmar, New insights into the biology and pathology of the cutaneous lymphatic system, J. Dermatol. Sci. 35 (2004) 1–8.
[4] H. Kubo, R. Cao, E. Brakenhielm, T. Makinen, Y. Cao, K. Alitalo, Blockade of vascular endothelial growth factor receptor-3 signaling inhibits fibroblast growth factor-2-induced lymphangiogenesis in mouse cornea, Proc. Natl. Acad. Sci. USA 99 (2002) (2002) 8868–8873.
[5] L.K. Chang, G. Garcia-Cardena, F. Farnebo, M. Fannon, E.J. Chen, C. Butterfield, M.A. Moses, R.C. Mulligan, J. Folkman, A. Kaipainen, Dose-dependent response of FGF-2 for lymphangiogenesis, Proc. Natl. Acad. Sci. USA 101 (2004) 11658–11663.
[6] P. Saharinen, P.T. Tammela, M.J. Karkkainen, K. Alitalo, Lymphatic vasculature: development molecular regulation and role in tumor metastasis and inflammation, Trends Immunol. 25 (2004) 387–395.
[7] A. Ristimaki, K. Narko, B. Enholm, V. Joukov, K. Alitalo, Proinflammatory cytokines regulate expression of the lymphatic endothelial mitogen vascular endothelial growth factor-C, J. Biol. Chem. 273 (1998) 8413–8418.
[8] M. Ryuto, M. Ono, H. Izumi, S. Yoshida, H.A. Weich, K. Kohno, M. Kuwano, Induction of vascular endothelial growth factor by tumor necrosis factor-alpha in human glioma cells: possible roles of Sp-1, J. Biol. Chem. 271 (1996) 28220–28228.
[9] S. Yoshida, M. Ono, T. Shono, H. Izumi, T. Ishibashi, H. Suzuki, M. Kuwano, Involvement of interleukin-8, vascular endothelial growth factor, and basic fibroblast growth factor in tumor necrosis factor alpha-dependent angiogenesis, Mol. Cell. Biol. 17 (1997) 4015–4023.
[10] M.R. Saban, S. Memet, D.G. Jackson, J. Ash, A.A. Roig, A. Israel, R. Saban, Visualization of lymphatic vessels through NF-kappaB activity, Blood 104 (2004) 3228–3230.
[11] P. Hamrah, L. Chen, Q. Zhang, M.R. Dana, Novel expression of vascular endothelial growth factor (VEGFR-3) and VEGF-C on corneal dendritic cells, Am. J. Pathol. 163 (2003) 57–68.
[12] P. Baluk, T. Tammela, E. Ator, N. Lyubynska, M.G. Achen, D.J. Hicklin, M. Jeltsch, T.V. Petrova, B. Pytowski, S.A. Stacker, S. Yla-Herttuala, D.G. Jackson, K. Alitalo, D.M. McDonald, Pathogenesis of persistent lymphatic vessel hyperplasia in chronic airway inflammation, J. Clin. Invest. 115 (2005) 247–257.
[13] M. Ono, Molecular links between tumor angiogenesis and inflammation: inflammatory stimuli of macrophages and cancer cells as targets for therapeutic strategy, Cancer Sci. 99 (2008) 1501–1506.
[14] C.A. Dinarello, Biologic basis for interleukin-1 in disease, Blood 87 (1996) 2095–2147.
[15] H. Torisu, M. Ono, H. Kiryu, M. Furue, Y. Ohmoto, J. Nakayama, Y. Nishioka, S. Sone, M. Kuwano, Macrophage infiltration correlates with tumor stage and angiogenesis in human malignant melanoma: possible involvement of TNF alpha and IL-1 alpha, Int. J. Cancer 85 (2000) 182–188.
[16] T. Kuwano, S. Nakao, H. Yamamoto, M. Tsuneyoshi, T. Yamamoto, M. Kuwano, M. Ono, Cyclooxygenase 2 is a key enzyme for inflammatory cytokine induced angiogenesis, FASEB J. 18 (2004) 300–310.
[17] S. Nakao, T. Kuwano, C. Tsutsumi-Miyahara, S. Ueda, Y.N. Kimura, S. Hamano, K. Sonoda, Y. Saijo, T. Nukiwa, R.M. Strieter, T. Ishibashi, M. Kuwano, M. Ono, Infiltration of COX2-expressing macrophages is a prerequisite for IL-1β-induced neovascularization and tumor growth, J. Clin. Invest. 115 (2005) 2979–2991.
[18] S. Nakao, Y. Hata, M. Miura, K. Noda, Y. Kimura, Y.S. Kawahara, T. Kita, T. Hisatomi, T. Nakazawa, Y. Jin, R. Dana, M. Kuwano, M. Ono, T. Ishibashi, A. Hafezi-Moghadam, Dexamethasone inhibits IL-1β-induced corneal neovascularization: role of NF-κB-activated stromal cells in inflammatory angiogenesis, Am. J. Pathol. 171 (2007) 1058–1065.
[19] C. Cursiefen, L. Chen, M.R. Dana, J.W. Streilein, Corneal lymphangiogenesis: evidence, mechanisms, and implications for corneal transplant immunology, Cornea 22 (2003) 273–281.
[20] T. Nakano, Y. Nakanishi, Y. Yonemitsu, S. Sumiyoshi, Y.X. Chen, Y. Akishima, T. Ishii, M. Iida, K. Sueishi, Angiogenesis and lymphangiogenesis and expression of lymphangiogenic factors in the atherosclerotic intima of human coronary arteries, Hum. Pathol. 36 (2005) 330–340.
[21] K. Matsumura, M. Hirashima, M. Ogawa, H. Kubo, H. Hisatsune, N. Kondo, S. Nishikawa, T. Chiba, S. Nishikawa, Modulation of VEGFR-2-mediated endothelial-cell activity by VEGF-C/VEGFR-3, Blood 101 (2003) 1367–1374.
[22] T. Makinen, T. Veikkola, S. Mustjoki, T. Karpanen, B. Catimel, E.C. Nice, L. Wise, A. Mercer, H. Kowalski, D. Kerjaschki, S.A. Stacker, M.G. Achen, K. Alitalo, Isolated lymphatic endothelial cells transduce growth, survival and migratory signals via the VEGF-C/D receptor VEGFR-3, EMBO J. 20 (2001) 4762–4773.
[23] S.I. Zittermann, A.C. Issekuts, Endothelial growth factors VEGF and bFGF differentially enhance monocyte and neutrophil recruitment to inflammation, J. Leukoc. Biol. 80 (2006) 247–257.
[24] Y. Kimura, K. Watari, A. Fotovati, F. Hosoi, K. Yasumoto, H. Izumi, K. Kohno, K. Umezawa, H. Iguchi, K. Shirouzu, S. Takamori, M. Kuwano, M. Ono, Inflammatory stimuli from macrophages and cancer cells synergistically promote tumor growth and angiogenesis, Cancer Sci. 98 (2007) 2009–2018.

(Selected as an issue highlight and a cover page.)

Azaspirene, a fungal product, inhibits angiogenesis by blocking Raf-1 activation

Yukihiro Asami,[1,5] Hideaki Kakeya,[1,6] Yusuke Komi,[2] Soichi Kojima,[2] Kiyohiro Nishikawa,[3] Kristin Beebe,[4] Len Neckers[4] and Hiroyuki Osada[1,7]

[1]Antibiotics Laboratory, Advanced Science Institute, RIKEN, 2-1 Hirosawa, Wako, Saitama 351-0198; [2]Molecular Cellular Pathology Research Unit, RIKEN, 2-1 Hirosawa, Wako, Saitama 351-0198; [3]R. and D. Division, Pharmaceuticals Group, Nippon Kayaku, 31-12 Shimo 3-chome, Kita-ku, Tokyo 115-8588, Japan; [4]Urologic Oncology Branch, National Cancer Institute, 9000 Rockville Pike, Building 10/CRC, 1-5940, Bethesda, Maryland 20892, USA

(Received January 18, 2008/Revised May 15, 2008/Accepted May 21, 2008/Online publication July 10, 2008)

Angiogenesis is an inevitable event in tumor progression and metastasis, and thus has been a compelling target for cancer therapy in recent years. Effective inhibition of tumor progression and metastasis could become a promising way to treat tumor-induced angiogenesis. We discovered that a fungus, *Neosartorya* sp., isolated from a soil sample, produced a new angiogenesis inhibitor, which we designated azaspirene. Azaspirene was previously shown to inhibit human umbilical vein endothelial cell (HUVEC) migration induced by vascular endothelial growth factor (VEGF) at an effective dose, 100% of 27 μmol/L without significant cell toxicity. In the present study, we investigated the antiangiogenic activity of azaspirene *in vivo*. Azaspirene treatment reduced the number of tumor-induced blood vessels. Administration of azaspirene at 30 μg/egg resulted in inhibition of angiogenesis (23.6–45.3% maximum inhibition relative to the controls) in a chicken chorioallantoic membrane assay. Next, we elucidated the molecular mechanism of antiangiogenesis of azaspirene. We investigated the effects of azaspirene on VEGF-induced activation of the mitogen-activated protein kinase signaling pathway in HUVEC. *In vitro* experiments indicated that azaspirene suppressed Raf-1 activation induced by VEGF without affecting the activation of kinase insert domain-containing receptor/fetal liver kinase 1 (VEGF receptor 2). Additionally, azaspirene preferentially inhibited the growth of HUVEC but not that of the non-vascular endothelial cells NIH3T3, HeLa, MSS31, and MCF-7. Taken together, these results demonstrate that azaspirene is a novel inhibitor of angiogenesis and Raf-1 activation that contains a unique carbon skeleton in its molecular structure. (*Cancer Sci* 2008; 99: 1853–1858)

The angiogenic process is tightly controlled by a wide variety of positive and negative regulators, including growth factors, cytokines, lipid metabolites, and cryptic fragments of hemostatic proteins.[1] Among these molecules, vascular endothelial growth factor (VEGF), a soluble angiogenic factor produced by many tumor and normal cells, plays a key role in regulating normal and abnormal angiogenesis.[2] Angiogenesis is also initiated in response to certain pathological conditions, such as solid tumor growth, diabetic retinopathy, psoriasis, and rheumatoid arthritis, in all of which angiogenesis is responsible for the disease progression.[3]

In particular, it is well-known that the growth of tumors larger than a few cubic millimeters requires continuous recruitment of new blood vessels.[4] Complex and diverse cellular actions are implicated in angiogenesis, namely extracellular matrix degradation, proliferation and migration of endothelial cells, and morphological differentiation of endothelial cells to form tubes.[3] These newly synthesized blood vessels also provide a route for cancer cells to enter the blood circulation and spread to other organs.[5] Therefore, the inhibition of angiogenesis is a promising strategy to treat tumors. In particular, research on VEGF receptors (VEGFR) has been a focus of angiogenesis research. VEGFR1 is required for the recruitment of hematopoietic precursors and for migration of monocytes and macrophages,[6] whereas VEGFR2 and VEGFR3 are essential for vascular endothelial and lymphendothelial cells, respectively.[7,8] Notably, the VEGFR2 signaling pathway is a promising target for inhibiting angiogenesis because it is a common pathway for tumor-induced angiogenesis.[9,10]

Especially, Raf-1 or Raf-1-interacting molecules are possible targets for antiangiogenic compounds.[11,12] In fact, various synthetic compounds that inhibit the VEGF, platelet-derived growth factor (PDGF), and epidermal growth factor (EGF) signaling pathways are under development, such as, vatalanib (PTK787/ZK222584), sorafenib (BAY 43-9006), and vandetanib (ZD6474/Zactima).[13–17] However, there have been relatively few reports of natural compounds with antiangiogenic activities.[18]

Hence, it is still important to explore new angiogenesis inhibitors from natural compounds. We have discovered several naturally occurring angiogenesis inhibitors, such as RK-805,[19] epoxyquinol A and B,[20,21] epoxytwinol A,[22] RK-95113,[23] and azaspirene, which has a 1-oxa-7-azaspiro[4.4]non-2-ene-4,6-dione skeleton and is derived from fungal metabolites.[24] In the present study, we report the antiangiogenic activity of azaspirene *in vivo* and reveal the molecular basis underlying it.

Materials and Methods

Reagents and antibodies. Azaspirene was prepared as described previously.[24] The selective kinase insert domain-containing receptor/fetal liver kinase 1 (KDR/Flk-1) tyrosine kinase inhibitor SU5614, MEK1 kinase inhibitor PD98059, and Hsp90 inhibitor geldanamycin were purchased from Calbiochem (La Jolla, CA, USA). Paclitaxel was purchased from Xi'an High-Tech Industries (Xian, China). Recombinant human VEGF was purchased from R & D Systems (Minneapolis, MN, USA). Recombinant human EGF, basic fibroblast growth factor (bFGF), and PDGF were purchased from Sigma-Aldrich (St Louis, MO, USA). Mouse monoclonal antibodies against phospho-tyrosine, MEK1, and MEK2 were purchased from Transduction Laboratories (Lexington, KY, USA), whereas antibodies against HSP90, Raf-1, phospho-Raf-1, phospho-ERK1/2, and phospho-MEK1/2 were purchased from Stressgen Biotechnologies (Victoria, BC, Canada), Santa Cruz Biotechnology (Santa Cruz, CA, USA), Upstate Biotechnology (Lake Placid, NY, USA), Cell Signaling Technology (Beverly, MA, USA), and Cell Signalling Technology, respectively. Rabbit

[5]Present address: Laboratory of Microbiology, Graduate School of Pharmaceutical Sciences, The University of Tokyo, 3-1, 7-chome, Hongo, Bunkyo-ku, Tokyo 113-0033, Japan.
[6]Present address: Department of System Chemotherapy and Molecular Sciences, Division of Bioinformatics and Chemical Genomics, Graduate School of Pharmaceutical Sciences, Kyoto University, 46-29 Yoshida-Shimoadachi, Sakyo-ku, Kyoto 606-8501, Japan.
[7]To whom correspondence should be addressed. E-mail: hisyo@riken.jp

doi: 10.1111/j.1349-7006.2008.00890.x

polyclonal antibodies against KDR/Flk-1, Raf-1, ERK1/2, and MEK1/2 were purchased from Santa Cruz Biotechnology, Zymed Laboratories (South San Francisco, CA, USA), Cell Signaling Technology, respectively. Blocking buffer and working concentrations of the above antibodies were prepared according to the manufacturers' instructions.

***In vivo* tumor-induced angiogenesis in a renal carcinoma xenograft model.** The assay for tumor-induced angiogenesis was carried out as described by Kreisle and Ershler.[25] Female BALB/c mice (7 weeks old; Charles River Laboratories, Tokyo, Japan) were used for *in vivo* experiments. BALB/c mice were injected intradermally (i.d.) with 1×10^6 murine renal carcinoma (RENCA) cells in the back on day 0. Mice were administered vehicle or paclitaxel (6 or 20 mg/kg, intraperitoneally [i.p.], daily) consisting of 5% ethanol and 5% polyoxyethylene castor oil in saline for days 0–6. Azaspirene was dissolved in normal saline containing 10% dimethyl sulfoxide (DSMO). Azaspirene (31.6 or 100 mg/kg, i.p.) was administered every second day (days 0, 2, 4, and 6). The animals were euthanized on day 7, and skin with tumors was separated from the underlying tissue. Tumor angiogenesis was quantified by counting the number of blood vessels oriented toward the tumor using a digital camera. The same observer made all counts. The present study was in accordance with the Helsinki Declaration of the World Medical Association and the guidelines of the ethical committees of the authors' institutions.

Chicken chorioallantoic membrane assay. The formation of new blood vessels within chicken chorioallantoic membrane (CAM) was assessed as described previously.[26] In brief, fertilized Dekalb chicken eggs (Omiya Kakin, Saitama, Japan) were placed in a humidified egg incubator. After a 4.5-day incubation at 38°C, a 1% solution of methylcellulose containing 30 μg azaspirene/egg was loaded inside a silicon ring placed on the surface of the CAM. After further incubation for 2 days, a fat emulsion was injected into the chorioallantois, such that the vascular networks stood out against the white background of the lipid. Antiangiogenic responses were evaluated under a stereomicroscope and photographed with a ×7.25 objective. Quantitative analyses were carried out with angiogenesis-measuring software (Kurabo Angiogenesis Image Analyzer, version 1.0; Kurabo, Osaka, Japan). Five eggs were analyzed in each treatment group, and all experiments were repeated three times.

Cell culture. MCF-7 cells were cultured in RPMI-1640 medium supplemented with 5% calf serum in the presence of 30 μg/mL penicillin and 42 μg/mL streptomycin under a humidified atmosphere of 5% CO_2 at 37°C. NIH3T3, HeLa, MSS31 (a mouse spleen stromal cell line; a gift from Dr. N. Yanai, Tohoku University), and HEK293T cells were cultured in Dulbecco's Modified Eagle's Medium containing 10% fetal calf serum (FCS) in 5% CO_2 at 37°C. Human umbilical vein endothelial cells (HUVEC) were cultured in Humedia-EG2 (Kurabo) at 37°C under a 5% CO_2 atmosphere. All cell experiments were carried out using HUVEC between passages three and six.

Western blotting. Pre-confluent NIH3T3, HeLa, MSS31, and MCF-7 cells were pretreated with serum-free medium. HUVEC were pretreated with M199 containing 2% FCS overnight and were left untreated or exposed to various concentrations of azaspirene for 60 min prior to the addition of various stimulators: VEGF (12.5 ng/mL), EGF (10 ng/mL), bFGF (10 or 25 ng/mL), PDGF (30 ng/mL), or phorbol 12, 13-dibutyrate (PDBu) (10 ng/mL). Twenty-five μmol/L PD98059 and 10 μmol/L SU5614 were used as a positive control for the MEK1 kinase inhibitor and the KDR/Flk-1 tyrosine kinase inhibitor, respectively. Western blotting experiments were prepared as described previously.[27,28]

Immunoprecipitation. Confluent HUVEC were pretreated with M199 containing 2% FCS medium overnight and were left untreated or exposed to various concentrations of azaspirene for 60 min prior to the addition of VEGF (12.5 ng/mL). SU5614 (10 μmol/L) and geldanamycin (10 μmol/L) were used as positive controls for KDR/Flk-1 tyrosine kinase inhibitor and Hsp90 inhibitor, respectively. The immunoprecipitation experiments were carried out as described previously.[29,30]

Cell proliferation assay. NIH3T3, HeLa, MSS31, MCF-7 and HUVEC were seeded on 96-well microplates (3.0×10^3 cells per well). Test compounds were dissolved in DMSO at appropriate concentrations and were treated for 48 h. Cell proliferation assays were carried out using the WST-8 (Nacalai Tesque, Kyoto, Japan) protocol. The absorbance (A_{450}) of each well was measured using a Wallac 1420 multilabel counter (Amersham Bioscience, Piscataway, NJ, USA).

Cell transfection. The expression plasmids bearing cDNA of KDR/Flk-1 were prepared as described previously.[31] We cloned the complementary DNA of KDR/Flk-1 into the *Kpn*I–*Xho*I sites of the pcDNA4/TO vector (Invitrogen, Carlsbad, CA, USA). Transfection of pcDNA4/TO-KDR/Flk-1 plasmids was carried out using Fugene HD (Roche Diagnostics, Mannheim, Germany) according to the manufacturer's standard protocol.

Results

Azaspirene inhibited tumor-induced angiogenesis in a renal carcinoma xenograft model. As azaspirene (Fig. 1a) was isolated from fungal metabolites by screening with an endothelial cell migration assay, the inhibitory activity of azaspirene against tumor-induced angiogenesis was examined using murine RENCA cells *in vivo*. BALB/c mice received either azaspirene (31.6 or 100 mg/kg, i.p., every second day) or paclitaxel (6 or 20 mg/kg, i.p., daily) after inoculation of RENCA cells (1×10^6 cells/site) subcutaneously. The number of vessels oriented toward the tumor, the tumor volume, and the bodyweight were assessed after 7 days. As shown in Fig. 1b,c, the number of blood vessels oriented toward the tumor decreased with azaspirene treatment. The maximum dose of 100 mg/kg also showed a tendency to reduce the tumor volume. Although the reduction in tumor volume did not reach statistical significance, in contrast to paclitaxel, the antiangiogenic activity of azaspirene was not associated with a loss of bodyweight (data not shown). These results clearly indicate that azaspirene had antiangiogenic effects *in vivo*.

Azaspirene showed antiangiogenic activity in a chicken CAM assay. The antiangiogenic activity of azaspirene was investigated *in vivo* using a chicken CAM assay. After 2 days of incubation, azaspirene elicited an antiangiogenic response, which was visible under a microscope as a spoke-wheel-like pattern of blood vessels. Azaspirene produced a decrease in the development of angiogenesis in the chick embryo without any sign of thrombosis or hemorrhage (Fig. 2a). In Fig. 2b, azaspirene suppressed the neovascularization of chick embryo when compared to vehicle ($71.4 \pm 18.1\%$ of the value obtained with 10% DMSO, $n = 5$ in each group).

Azaspirene inhibited angiogenic factor-induced activation of MAPK in HUVEC. VEGF induces proliferation and migration through activation of its cell surface receptor, KDR/Flk-1.[32] To understand the molecular mechanism by which azaspirene exerts its antiangiogenic activities, we investigated the effects of azaspirene on VEGF-induced activation of MEK1/2 and ERK1/2, which are downstream signaling molecules of KDR/Flk-1. VEGF-induced MEK1/2 and ERK1/2 activations were significantly inhibited by azaspirene in a dose-dependent manner (Fig. 3a), and azaspirene suppressed the kinase cascade Raf-1–MEK–ERK pathway activated by three other stimulation factors, EGF, bFGF, and PDBu (Fig. 3b–d). These data suggest that azaspirene blocks upstream activation of the MAP kinase signaling pathway in HUVEC.

Azaspirene inhibited VEGF-induced Raf-1 activation without affecting tyrosine phosphorylation of KDR/Flk-1 or protein complexes of Raf-1. To examine the effect of azaspirene on the cellular mechanism of Raf-1 activation, formation of Raf-1 complexes, and phosphorylation of KDR/Flk-1 in HUVEC, we studied the

doi: 10.1111/j.1349-7006.2008.00890.x

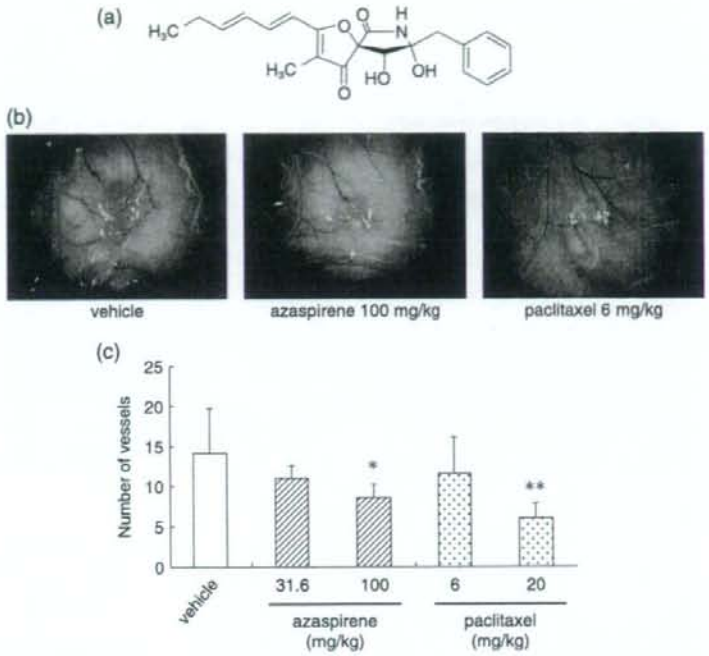

Fig. 1. Effect of azaspirene on tumor-induced angiogenesis *in vivo*. (a) The chemical structure of azaspirene. (b) Photographs of tumor-induced vessel formation after treatment with vehicle, azaspirene, and paclitaxel. (c) Quantification of newly formed blood vessels. The statistical significance of differences between the control and experimental groups was determined using one-way ANOVA, Tukey method analysis, repeated measures. $*P < 0.05$; $**P < 0.01$ was taken as the level of statistical significance.

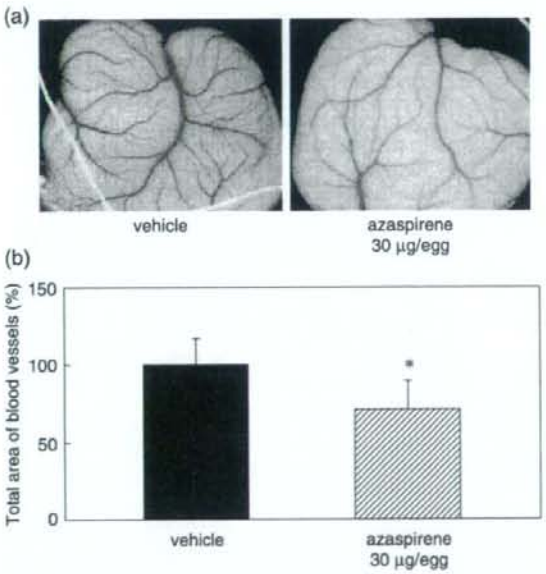

Fig. 2. Suppression of blood vessel formation within chorioallantoic membrane (CAM) by azasprirene. (a) The 4.5-day-old CAM were treated with increasing concentrations of azaspirene for 48 h, and then patterns of angiogenesis were photographed. (b) The total area of blood vessels was analyzed with angiogenesis-measuring software and is shown under each panel. Solid column, vehicle (10% dimethyl sulfoxide); hatched column, 30 μg/egg azaspirene. The statistical significance of differences between control and experimental groups was determined using two-group two-tailed Student's *t*-test. $*P < 0.05$ was taken as the level of statistical significance.

phosphorylation of Raf-1 and Raf-1-binding proteins. The results showed that azaspirene inhibited VEGF-induced phosphorylation of Raf-1 in a dose-dependent manner (Fig. 4a). Additionally, azaspirene had no effect on the disruption of Hsp90–Raf-1–MEK complexes and did not markedly suppress VEGF-induced KDR/Flk-1 autophosphorylation at concentrations up to 81 μmol/L (Fig. 4a,b). These data suggest that the mode of action of azaspirene is different from those of known antiangiogenic compounds, such as the receptor tyrosine kinase inhibitor, vatalanib, Raf-1 kinase inhibitor, and sorafenib.[13–17]

Azaspirene did not inhibit angiogenic factor-induced activation of ERK1/2 in NIH3T3, HeLa, MSS31, and MCF-7 cells. To investigate the effect of azaspirene on the activation of ERK1/2 in several cell lines other than HUVEC, we examined the phosphorylation of ERK1/2 in non-vascular endothelial cells. As shown in Fig. 5a, phosphorylation of ERK1/2 induced by bFGF, PDGF, and PDBu in NIH3T3 cells was not remarkably suppressed by azaspirene at 81 or 270 μmol/L. Similarly, azaspirene did not inhibit the phosphorylation of ERK1/2 induced by EGF or PDBu in HeLa, MSS31, or MCF-7 cells (Fig. 5b,c). These results suggest that azaspirene specifically inhibits the MAPK signaling pathway in vascular endothelial cells.

Azaspirene preferentially inhibited the growth of HUVEC and suppressed MAPK activation in HEK293T cells transiently expressing KDR/Flk-1. To investigate the effect of azaspirene on cell growth inhibition and MAPK activation in HEK293T cells transiently expressing KDR/Flk-1, we examined the unique biological activities of azaspirene on HUVEC. We first tested the effects of azaspirene on the growth of NIH3T3, HeLa, MSS31, MCF-7, and HUVEC in a proliferation assay. Interestingly, azaspirene preferentially inhibited the growth of HUVEC rather than those of the other four cell lines at 81.4 μmol/L (Fig. 6a). In addition, we investigated whether azaspirene influenced VEGF-triggered activation of the MAPK signaling pathway in HEK293T cells transiently expressing KDR/Flk-1.[33] VEGF-induced ERK1/2 activation was strongly inhibited by azaspirene at 27 μmol/L

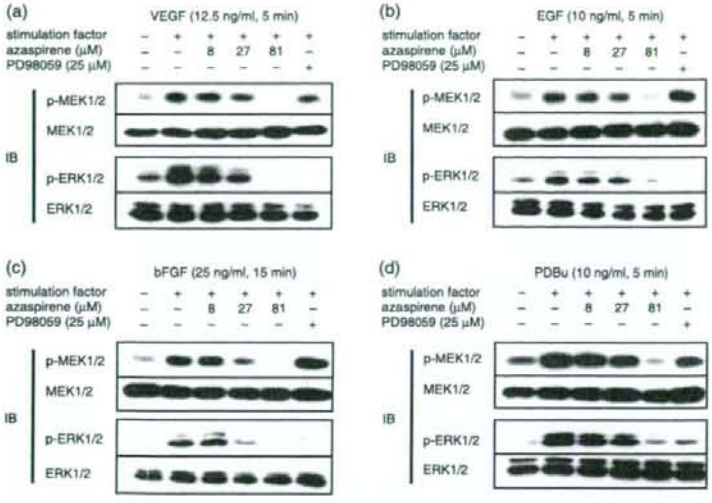

Fig. 3. Effect of azaspirene on the mitogen-activated protein (MAP) kinase signaling pathways in human umbilical vein endothelial cells (HUVEC). Azaspirene inhibited the phosphorylation of MEK1 and 2 and ERK1 and 2 induced by (a) vascular endothelial growth factor (VEGF), (b) epidermal growth factor (EGF), (c) basic fibroblast growth factor (bFGF), and (d) phorbol 12, 13-dibutyrate (PDBu). HUVEC were pretreated for 60 min with various concentrations (8, 27, or 81 μmol/L) of azaspirene and PD98059 (25 μmol/L) before exposure to VEGF (12.5 ng/mL) for 5 min, EGF (10 ng/mL) for 5 min, bFGF (25 ng/mL) for 15 min, or PDBu (10 ng/mL) for 5 min. After stimulation the cells were harvested and western blotting was carried out. IB, antibodies used for western blotting. The results shown are representative of three experiments.

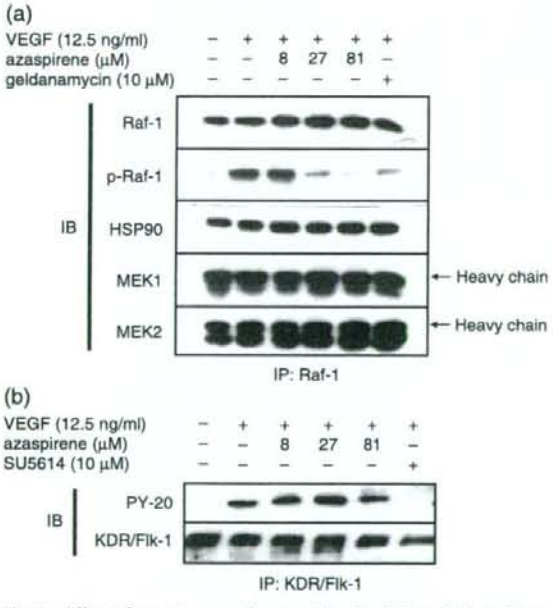

Fig. 4. Effect of azaspirene on the autophosphorylation of kinase insert domain-containing receptor/fetal liver kinase 1 (KDR/Flk-1), phosphorylation of Raf-1, and disruption of Raf-1 complexes. (a) Azaspirene did not inhibit the autophosphorylation of KDR/Flk-1 induced by vascular endothelial growth factor (VEGF). Human umbilical vein endothelial cells (HUVEC) were pretreated for 60 min with various concentrations (8, 27, or 81 μmol/L) of azaspirene and SU5614 (10 μmol/L) before exposure to VEGF (12.5 ng/mL) for 5 min. (b) Azaspirene inhibited the phosphorylation of Raf-1 induced by VEGF (12.5 ng/mL, 5 min), but did not disrupt the Raf-1, Hsp90, MEK1, or MEK2 complexes. HUVEC were pretreated for 60 min with various concentrations (8, 27, or 81 μmol/L) of azaspirene and geldanamycin (10 μmol/L) before exposure to VEGF (12.5 ng/mL) for 5 min. IB, western blotting analysis; IP, immunoprecipitation experiments. The results shown are representative of three experiments.

(Fig. 6b). These results demonstrate that azaspirene has a unique biological activity of preferentially inhibiting the growth of HUVEC and would inhibit ERK1/2 activation in cells expressing KDR/Flk-1 in a specific manner.

Discussion

Recently, Igarashi *et al.* reported the antiangiogenic activity of fluorosynerazol, which possesses a 1-oxa-7-azaspiro[4.4]non-2-ene-4,6-dione skeleton identical to azaspirene.[34] Fluorosynerazol showed an antiangiogenic effect in a CAM assay, but its mode of action was not elucidated. As both fluorosynerazol and azaspirene had the same oxo-azaspiro skeleton, we sought to reveal the molecular target of azaspirene, which appeared to inhibit only new tumor-induced blood vessel formation without having any visible effect on preexisting blood vessels (Fig. 1b).

The antiangiogenic activity of azaspirene was confirmed using both a tumor neo-angiogenesis assay (Fig. 1) and a CAM assay (Fig. 2). Next, we focused on identifying the molecular target of azaspirene and investigated the effects of azaspirene on VEGF-induced activation of the MAPK signaling pathway in HUVEC. We observed that azaspirene was capable of blocking the downstream events of VEGF-induced KDR/Flk-1 signaling, such as activation of MEK1/2 and ERK1/2. We also found that azaspirene inhibited EGF-, bFGF-, and PDBu-induced MEK1/2 and ERK1/2 activations at a similar concentration as used for VEGF in HUVEC. Azaspirene inhibited the VEGF-induced phosphorylation of ERK1/2 in mouse endothelial MS1 VEGF cells (data not shown). It is suggested that azaspirene possesses interesting properties, such as preferential interference with VEGF-induced MAPK signaling in HUVEC.

Azaspirene suppressed VEGF-induced Raf-1 activation without affecting the activation of KDR/Flk-1 or disrupting Hsp90–Raf-1–MEK1–MEK2 complexes in HUVEC. Moreover, we found that this activity of azaspirene was not due to Hsp90 inhibition (data not shown). Thus, azaspirene specifically blocked VEGF-induced phosphorylation of Raf-1, but the molecular target through which it exerts its effects remains unknown. There are controversial reports on Raf-1 activation in endothelial cells. One research group suggested Ras-independent Raf-1 activation via a protein kinase C (PKC)-dependent pathway.[29,35,36] Another group suggested the involvement of p21-activated protein kinase-1 and src kinase on Raf-1 activation.[37–39] To clarify the

doi: 10.1111/j.1349-7006.2008.00890.x

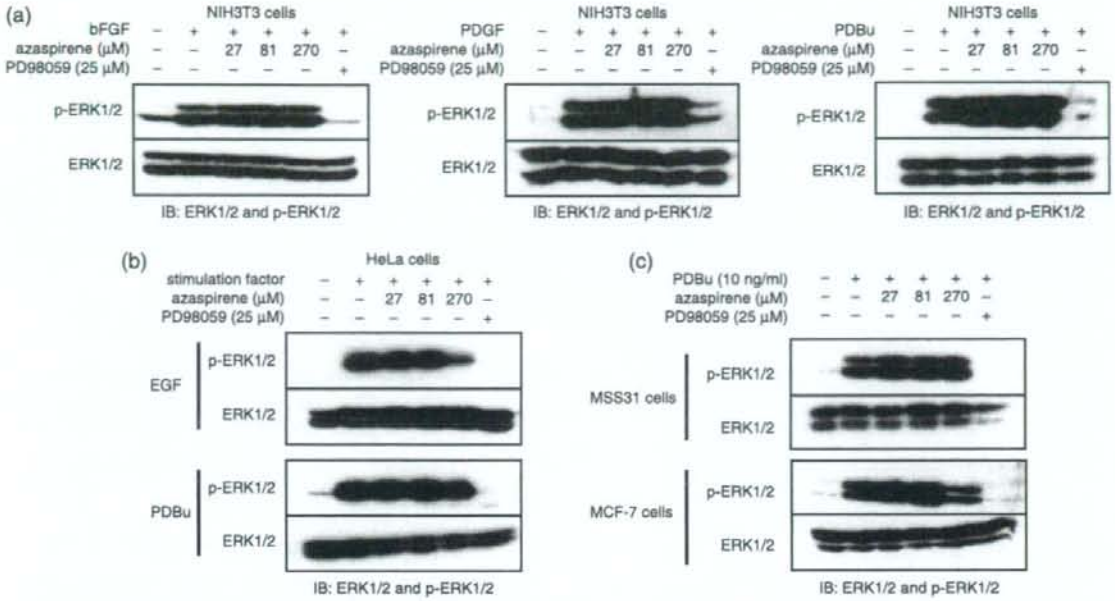

Fig. 5. Effect of azaspirene on the mitogen-activated protein (MAP) kinase signaling pathways in NIH3T3, HeLa, MSS31, and MCF-7 cells. Azaspirene did not inhibit the phosphorylation of ERK1 and 2 induced by platelet-derived growth factor (PDGF), epidermal growth factor (EGF), or phorbol 12, 13-dibutyrate (PDBu) in other cell lines. (a) NIH3T3 cells were pretreated for 60 min with various concentrations (27, 81, or 270 μmol/L) of azaspirene and PD98059 (25 μmol/L) before exposure to basic fibroblast growth factor (bFGF) (10 ng/mL) for 5 min, PDGF (30 ng/mL) for 5 min, or PDBu (10 ng/mL) for 5 min. (b) Azaspirene did not inhibit the phosphorylation of ERK1 and 2 induced by EGF (10 ng/mL, 5 min) or PDBu (10 ng/mL, 5 min) in HeLa cells. (c) MSS31 and MCF-7 cell lines were pretreated for 60 min with various concentrations (27, 81, or 270 μmol/L) of azaspirene and PD98059 (25 μmol/L) before exposure to PDBu (10 ng/mL) for 5 min. After stimulation, the cells were harvested and western blotting was carried out. IB, western blotting analysis. The results shown are representative of three experiments.

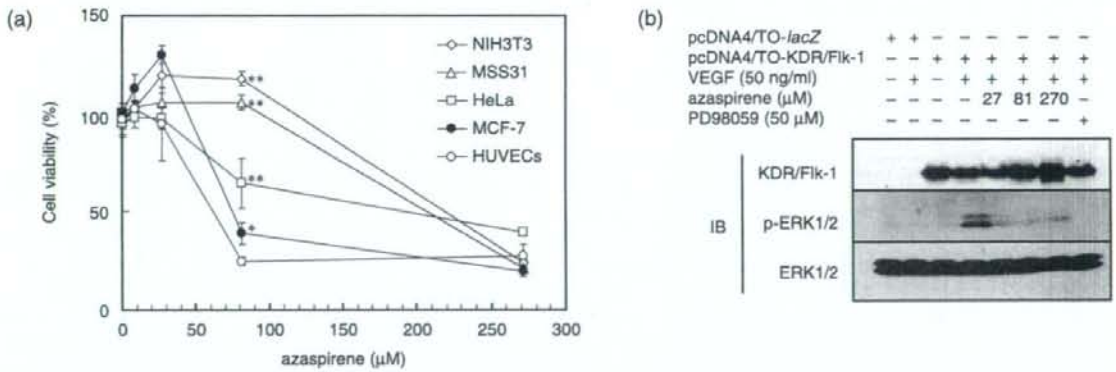

Fig. 6. Effects of azaspirene on the growth of human umbilical vein endothelial cells (HUVEC) and on mitogen-activated protein kinase (MAPK) activation in the HEK293T cell system. (a) Effects of azaspirene on the growth of NIH3T3, HeLa, MSS31, and MCF-7 cells and HUVEC in a proliferation assay. The azaspirene-induced growth inhibitions for the different cell lines were as follows: ◇, NIH3T3 (IC_{50} = 216 μmol/L); □, HeLa (IC_{50} = 189 μmol/L); △, MSS31 (IC_{50} = 173 μmol/L); ●, MCF-7 (IC_{50} = 75.6 μmol/L); and ○, HUVEC (IC_{50} = 62.1 μmol/L). Each value is expressed relative to the 1% dimethyl sulfoxide (DMSO) control group; bars, SD. The statistical significance of differences between the growth inhibition (%) of HUVEC with azaspirene at 81 μmol/L was determined using one-way ANOVA, Tukey method analysis, repeated measures. $^{*}P < 0.05$; $^{**}P < 0.01$ was taken as the level of statistical significance. (b) Effects of azaspirene on vascular endothelial growth factor (VEGF)-induced ERK1 and 2 phosphorylation in HEK293T cells expressing kinase insert domain-containing receptor/fetal liver kinase 1 (KDR/Flk-1). HEK293T cells transfected with KDR/Flk-1 were incubated for 1 h in the absence (DMSO) or presence of various concentrations of azaspirene (27, 81, or 270 μmol/L). These cells were then treated with 50 ng/mL VEGF for 5 min. After stimulation, the cells were harvested, and western blotting was carried out. IB, western blotting analysis. The results shown are representative of three experiments.

molecular mechanism of Raf-1 activation, we elucidated the mechanism of azaspirene.

It is noteworthy that azaspirene preferentially inhibited the cell growth of HUVEC when compared with NIH3T3, HeLa, MSS31, and MCF-7 cells (Fig. 6a). Next, we demonstrated that azaspirene inhibited the activation of ERK1/2 in KDR/Flk-1-overexpressing HEK293T cells (Fig. 6b). These results were consistent with the observation that azaspirene specifically inhibits the MAPK signaling pathway in HUVEC.

In conclusion, our current data demonstrate that azaspirene had antiangiogenic properties *in vivo*, and we have revealed that the effects of azaspirene on Raf-1 activation might be correlated with its antiangiogenic activity. Further intensive studies of the target identification of azaspirene will unravel the mystery of the VEGF-signaling pathway in HUVEC.

Acknowledgments

This work was supported in part by a Grant-in-Aid from the Ministry of Education, Culture, Sports, Science, and Technology of Japan, by a Grant-in-Aid for Cancer Research from the Ministry of Health, Labour, and Welfare of Japan, by the Chemical Biology Project (RIKEN), and by funding from the Special Postdoctoral Researchers Program (to Y. A.). The authors thank the Screening Committee of New Anticancer Agents, which is supported by a Grant-in-Aid for Scientific Research on the Priority Area 'Cancer' from The Ministry of Education, Culture, Sports, Science, and Technology of Japan. We are grateful to Ms. K. Kawai, Dr. Y. Tamura, Dr. S. Takahashi, and Dr. S. Simizu (RIKEN) for suggestions concerning the western blotting and immunoprecipitation experiments.

References

1 Bussolino F, Mantovani A, Persico G. Molecular mechanisms of blood vessel formation. *Trends Biochem Sci* 1997; **22**: 251–6.
2 Inser JM, Asahara T. Angiogenesis and vasculogenesis as therapeutic strategies for postnatal neovascularization. *J Clin Invest* 1999; **103**: 1231–6.
3 Hanhan D, Folkman J. Patterns and emerging mechanisms of the angiogenic switch during tumorigenesis. *Cell* 1996; **82**: 353–64.
4 Folkman J. What is the evidence that tumors are angiogenesis dependent? *J Natl Cancer Inst* 1990; **80**: 4–6.
5 Fidler IJ, Ellis LM. The implications of angiogenesis for the biology and therapy of cancer metastasis. *Cell* 1994; **79**: 185–8.
6 Murakami M, Iwai S, Hiratsuka S *et al.* Signaling of vascular endothelial growth factor receptor-1 tyrosine kinase promotes rheumatoid arthritis through activation of monocytes/macrophages. *Blood* 2006; **108**: 1849–56.
7 Shibuya M, Claesson-Welsh L. Signal transduction by VEGF receptors in regulation of angiogenesis and lymphangiogenesis. *Exp Cell Res* 2006; **312**: 549–60.
8 He Y, Rajantie I, Pajusola K *et al.* Vascular endothelial cell growth factor receptor 3-mediated activation of lymphatic endothelium is crucial for tumor cell entry and spread via lymphatic vessels. *Cancer Res* 2005; **65**: 4739–46.
9 Sridhar SS, Hedley D, Siu LL. Raf kinase as a target for anticancer therapeutics. *Mol Cancer Ther* 2005; **4**: 677–85.
10 Olsson AK, Dimberg A, Kreuger J, Claesson-Welsh L. VEGF receptor signalling – in control of vascular function. *Nat Rev Mol Cell Biol* 2006; **7**: 359–71.
11 Wilhelm SM, Carter C, Tang L *et al.* BAY 43-9006 exhibits broad spectrum oral antitumor activity and targets the RAF/MEK/ERK pathway and receptor tyrosine kinases involved in tumor progression and angiogenesis. *Cancer Res* 2004; **64**: 7099–109.
12 Dasgupta P, Sun J, Wang S *et al.* Disruption of the Rb–Raf-1 interaction inhibits tumor growth and angiogenesis. *Mol Cell Biol* 2004; **24**: 9527–41.
13 Xu L, Yoneda J, Herrera C, Wood J, Killion JJ, Fidler IJ. Inhibition of malignant ascites and growth of human ovarian carcinoma by oral administration of a potent inhibitor of the vascular endothelial growth factor receptor tyrosine kinases. *Int J Oncol* 2000; **16**: 445–54.
14 Lyons JF, Wilhelm S, Hibner B, Bollag G. Discovery of a novel Raf kinase inhibitor. *Endocr Relat Cancer* 2001; **3**: 219–25.
15 Hennequin LF, Stokes ES, Thomas AP *et al.* Novel 4-anilinoquinazolines with C-7 basic side chains: design and structure activity relationship of a series of potent, orally active, VEGF receptor tyrosine kinase inhibitors. *J Med Chem* 2002; **45**: 1300–12.
16 Duran I, Hotte SJ, Hirte H *et al.* Phase I targeted combination trial of sorafenib and erlotinib in patients with advanced solid tumors. *Clin Cancer Res* 2007; **13**: 4849–57.
17 Elser C, Siu LL, Winquist E *et al.* Phase II trial of sorafenib in patients with recurrent or metastatic squamous cell carcinoma of the head and neck or nasopharyngeal carcinoma. *J Clin Oncol* 2007; **25**: 3766–73.
18 Verheul HM, Pinedo HM. Possible molecular mechanisms involved in the toxicity of angiogenesis inhibition. *Nat Rev Cancer* 2007; **7**: 475–85.
19 Asami Y, Kakeya H, Onose R, Chang YH, Toi M, Osada H. RK-805, an endothelial-cell-growth inhibitor produced by *Neosartorya* sp. and a docking model with methionie aminopeptidase-2. *Tetrahedron* 2004; **60**: 7085–91.
20 Kakeya H, Onose R, Koshino H *et al.* Epoxyquinol A, a highly functionalized pentaketide dimer with antiangiogenic activity isolated from fungal metabolites. *J Am Chem Soc* 2002; **124**: 3496–7.
21 Kakeya H, Onose R, Yoshida A, Koshino H, Osada H. Epoxyquinol B, a fungal metabolite with a potent antiangiogenic activity. *J Antibiot* 2002; **55**: 829–31.
22 Kakeya H, Onose R, Koshino H, Osada H. Epoxytwinol A, a novel unique angiogenesis inhibitor with C2 symmetry, produced by a fungus. *Chem Commun* 2005; **20**: 2575–7.
23 Asami Y, Kakeya H, Okada G, Toi M, Osada H. RK-95113, a new angiogenesis inhibitor produced by *Aspergillus fumigatus*. *J Antibiot* 2006; **59**: 724–8.
24 Asami Y, Kakeya H, Onose R, Yoshida A, Matsuzaki H, Osada H. Azaspirene: a novel angiogenesis inhibitor containing a 1-oxa-7-azaspiro[4.4]non-2-ene-4,6-dione skeleton produced by the fungus *Neosartorya* sp. *Org Lett* 2002; **17**: 2845–8.
25 Kreisle R, Ershler W. Investigation of tumor angiogenesis in an id mouse model: role of host–tumor interactions. *J Natl Cancer Inst* 1988; **80**: 849–54.
26 Suzuki Y, Komi Y, Ashino H *et al.* Retinoic acid controls blood vessel formation by modulating endothelial and mural cell interaction via suppression of Tie2 signaling in vascular progenitor cells. *Blood* 2004; **104**: 166–9.
27 Simizu S, Tamura Y, Osada H. Dephosphorylation of Bcl-2 by protein phosphatase 2A results in apoptosis resistance. *Cancer Sci* 2004; **95**: 266–70.
28 Tamura Y, Simizu S, Osada H. The phosphorylation status and anti-apoptotic activity of Bcl-2 are regulated by ERK and protein phosphatase 2A on the mitochondria. *FEBS Lett* 2004; **569**: 249–55.
29 Takahashi T, Ueno H, Shibuya M. VEGF activates protein kinase C-dependent, but Ras-independent Raf–MEK–MAP kinase pathway for DNA synthesis in primary endothelial cells. *Oncogene* 1999; **18**: 2221–30.
30 Kanno S, Oda N, Abe M *et al.* Roles of two VEGF receptors, Flt-1 and KDR, in the signal transduction of VEGF effects in human vascular endothelial cells. *Oncogene* 2000; **19**: 2138–46.
31 Sasaki A, Taketomi T, Kato R *et al.* Sprouty4 suppresses Ras-independent ERK activation by binding to Raf1. *Nat Cell Biol* 2003; **5**: 427–32.
32 Tomanek RJ, Holifield JS, Reiter RS, Sandra A, Lin JJ. Role of VEGF family members and receptors in coronary vessel formation. *Dev Dyn* 2002; **225**: 233–40.
33 Kuriyama M, Taniguchi T, Shirai Y, Sasaki A, Yoshimura A, Saito N. Activation and translocation of PKCδ is necessary for VEGF-induced ERK activation through KDR in HEK293T cells. *Biochem Biophys Res Commun* 2004; **325**: 843–51.
34 Igarashi Y, Yabuta Y, Sekine A *et al.* Directed biosynthesis of fluorinated pseurotin A, synerazol and gliotoxin. *J Antibiot* 2004; **57**: 748–54.
35 Hood J, Granger HJ. Protein kinase G mediates vascular endothelial growth factor-induced Raf-1 activation and proliferation in human endothelial cells. *J Biol Chem* 1998; **273**: 23 504–8.
36 Takahashi T, Yamaguchi S, Chida K, Shibuya M. A single autophosphorylation site on KDR/Flk-1 is essential for VEGF-A-dependent activation of PLC-γ and DNA synthesis in vascular endothelial cells. *EMBO J* 2001; **20**: 2768–78.
37 Alavi A, Hood JD, Frausto R, Stupack DG, Cheresh DA. Role of Raf in vascular protection from distinct apoptotic stimuli. *Science* 2003; **301**: 94–6.
38 Hood JD, Frausto R, Kiosses WB, Schwartz MA, Cheresh DA. Differential αv integrin-mediated Ras–ERK signaling during two pathways of angiogenesis. *J Cell Biol* 2003; **162**: 933–43.
39 Chong H, Vikis HG, Guan KL. Mechanisms of regulating the Raf kinase family. *Cell Signal* 2003; **15**: 463–9.

doi: 10.1111/j.1349-7006.2008.00890.x

Biosci. Biotechnol. Biochem., **72** (7), 1894–1900, 2008

Epoxyquinol B, a Naturally Occurring Pentaketide Dimer, Inhibits NF-κB Signaling by Crosslinking TAK1

Hiroshi KAMIYAMA,[1,2] Takeo USUI,[3] Hiroaki SAKURAI,[4] Mitsuru SHOJI,[5,*] Yujiro HAYASHI,[5] Hideaki KAKEYA,[1,**] and Hiroyuki OSADA[1,2,†]

[1]*Antibiotics Laboratory, RIKEN Advanced Science Institute, 2-1 Hirosawa, Wako, Saitama 351-0198, Japan*
[2]*Graduate School of Science and Engineering, Saitama University, 255 Shimo-okubo, Sakura-ku, Saitama 338-8570, Japan*
[3]*Graduate School of Life and Environmental Sciences, University of Tsukuba, 1-1-1 Tennodai, Tsukuba, Ibaraki 305-8572, Japan*
[4]*Division of Pathogenic Biochemistry, Institute of Natural Medicine, University of Toyama, 2630 Sugitani, Toyama 930-0194, Japan*
[5]*Department of Industrial Chemistry, Faculty of Engineering, Tokyo University of Science, 1-3 Kagurazaka, Shinjuku-ku, Tokyo 162-8601, Japan*

Received March 6, 2008; Accepted April 14, 2008; Online Publication, July 7, 2008
[doi:10.1271/bbb.80142]

Several epoxyquinoids interfere with NF-κB signaling by targeting IKKβ or NF-κB. We report that epoxyquinol B (EPQB), classified as an epoxyquiniod, inhibits NF-κB signaling through inhibition of the TAK1 complex, a factor upstream of IKKβ and NF-κB. cDNA microarray analysis revealed that EPQB decreased TNF-α-induced expression of NF-κB target genes. EPQB covalently bound to a recombinant TAK1-TAB1 fusion protein *in vitro*, and inhibited its kinase activity. Furthermore, *in vitro/in situ* treatment with EPQB resulted in a ladder-like hypershift of TAK1 protein bands. We reported recently that EPQB crosslinks proteins *via* cysteine residues by opening its two epoxides, and our current results suggest that EPQB inhibits NF-κB signaling by crosslinking TAK1 itself or TAK1 through other proteins.

Key words: epoxyquinol B; crosslink; TAK1; NF-κB

Epoxyquinoids exert anti-inflammatory effects by inhibiting nuclear factor κB (NF-κB) signaling.[1] Dehydroxymethylepoxyquinomicin (DHMEQ) delivers anti-inflammatory and antitumor effects by inhibiting the nuclear translocation of NF-κB.[2] Jesterone dimer, which is structurally similar to epoxyquinols, also inhibits NF-κB activation.[3] Moreover, several epoxyquinoids, for example, parthenolide, a sesquiterpen lactone isolated from the medicinal herb *Feverfew*,[4] manumycin A, an antibiotic from *Streptomyces parvulus*,[5] and epoxyquinone A monomer, a synthetic derivative of epoxyquinol,[6] have been reported to inhibit I-κB kinase (IKK) β kinase activity.

These inhibitory activities are thought to be mediated by the epoxide structure of epoxyquinoids, which reacts with nucleophiles, especially cysteine thiol groups. Parthenolide, manumycin A, and epoxyquinone A monomer bind directly to Cys-179 of IKK β, which is in the activation loop and plays a critical role in enzyme activation.[7]

We have found that epoxyquinol B (EPQB), a fungal metabolite and an epoxyquinoid that contains two epoxides, inhibits angiogenesis by covalently binding to cysteine residues of VEGFR2, EGFR, FGFR, and PDGFRβ.[8] Furthermore, we recently found that EPQB crosslinks proteins through cysteine residues by opening its two epoxides.[9] Hence, we hypothesized that EPQB inhibits signal transduction, including NF-κB signaling, through inter- and intramolecular crosslinking of target proteins.

Here, we report that EPQB blocks tumor necrosis factor-α (TNF-α)-induced NF-κB signaling through inhibition of TAK1, which plays a critical role in activating NF-κB signals. Additionally, EPQB binds directly to a TAK1-TAB1 fusion protein and crosslinks this protein complex. These findings suggest that EPQB inhibits NF-κB signaling by crosslinking pro-

† To whom correspondence should be addressed. Fax: +81-48-462-4669; E-mail: hisyo@riken.jp
* Present address: *Department of Chemistry, Graduate School of Science, Tohoku University, 6-3 Aramaki-Aza, Aoba, Sendai 980-8578, Japan*
** Present address: *Department of System Chemotherapy and Molecular Science, Division of Bioinformatics and Chemical Genomics, Graduate School of Pharmaceutical Sciences, Kyoto University, 46-29 Yoshida-Shimoadachi, Sakyo-ku, Kyoto 606-8501, Japan*

teins, including TAK1 itself or TAK1 through other proteins.

Materials and Methods

Cells and reagents. HeLa cells were cultured in Dulbecco's Modified Eagle's Medium (Sigma, St. Louis, MO) containing 10% heat-inactivated fetal calf serum (FCS) (JRH Bioscience, Lenexa, KS), 50 units/ml of penicillin, and 50 μg/ml of streptomycin (Sigma). Human umbilical vein endothelial cells (HUVECs) were cultured in HuMedia-EG2 (Kurabo, Osaka, Japan) containing 2% FCS in 5% CO_2 at 37 °C. Isolation and total synthesis of EPQB were performed as described previously.[10] Biotinylated EPQB (Bio-EPQB) was synthesized by oxime formation from EPQB and biotinylated alkoxyamine, which was prepared from 1,8-diamino-3,6-dioxaoctane *via* seven chemical transformations. The structure of biotinylated EPQB was determined by its physico-chemical properties, detailed ^{1}H- and ^{13}C-NMR analyses including two-dimensional techniques, and mass spectroscopies. Recombinant human TNF-α was purchased from Sigma.

Antibodies. Anti-phospho-TAK1 (Thr-187) antibody was described previously.[11,12] Anti-p65 rabbit polyclonal antibody (F-6), anti-IκB-α rabbit polyclonal antibody (C-21), anti-TAB1 goat polyclonal antibody (C-20), anti-TAB2 goat polyclonal antibody (E-20), anti-TAK1 rabbit polyclonal antibody (M-579), and anti-RIP rabbit polyclonal antibody (K-20) were purchased from Santa Cruz Biotechnology (Santa Cruz, CA). Anti-phospho-I-κB-α rabbit polyclonal antibody (#9241), anti-IKKβ rabbit polyclonal antibody (#2684), and anti-phospho-IKKβ rabbit polyclonal antibody (#2694), were from Cell Signaling Technology (Beverly, MA).

cDNA microarray analysis. HUVECs (2×10^6 cells/well) were cultured and treated with and without EPQB for 2 h. After stimulation with TNF-α (20 ng/ml) for 1 h, total RNA was extracted using ISOGEN (Nippon Gene, Tokyo). Next, cDNA microarray analysis was performed using the cDNA GEArray Human NF-κB Signaling Kit (SuperArray, Frederick, MD). The gene expression profiles determining upregulation or downregulation of genes after EPQB treatment were compared using GEArray analyzer software (Super Array).

Immunofluorescence analysis. To investigate the localization of NF-κB p65, HeLa cells were incubated on glass coverslips with or without EPQB for 2 h and stimulated with 20 ng/ml of TNF-α for 40 min. Immunofluorescence analysis of NF-κB p65 was performed as described previously.[2] To quantify fluorescence localization in the nucleus, the numbers of p65-positive nuclei were counted. The data are the representative averages of triplicate experiments.

Plasmids and transfections. A Flag-tagged TAK1-expressing plasmid was transiently transfected into HeLa cells using the Fugene 6 transfection reagent (Roche Diagnostics, Germany). After 24 h of incubation, the transfected cells were treated with and without EPQB for 2 h and stimulated by TNF-α (20 ng/ml) for 5 min. The samples were analyzed by Western blotting.

Immunoprecipitation and Western blot analysis. HeLa cells and HEK293T cells (2×10^5 cell/well) were treated with and without EPQB for 2 h and stimulated with TNF-α (20 ng/ml) for 5 min. Immunoprecipitation and Western blot analysis were performed as described previously.[11,12] Proteins were visualized using the SuperSignal West Pico Chemiluminescent Substrate (Pierce, Rockford, IL).

TAK1 kinase assay. Human recombinant TAK1-TAB1 fusion protein (Upstate Biotechnology, Charlottesville, VA) and MKK6 (Jena Bioscience, Jena, Germany) were used in the TAK1 kinase assay. TAK1 kinase activity was analyzed as described.[11,12] The percentage of inhibition was quantified with a bioimage analyzer (Fujix BAS2000).

In vitro *binding assay.* In the *in vitro* competitive binding assay, human recombinant TAK1-TAB1 fusion protein (100 ng/sample) was incubated with and without 0.1, 1, and 10 mM EPQB for 1 h at 37 °C in 50 mM Tris–HCl (pH 7.4). Next, each sample was treated with biotinylated EPQB (Bio-EPQB) 8) at 0.5 mM for 1 h at 37 °C. These samples were detected by Western blotting.

Results

EPQB downregulates expression of NF-κB target genes

Natural and synthetic epoxyquinoids have been reported to inhibit NF-κB signaling.[1] Hence, we investigated the effects of EPQB on NF-κB signaling by measuring changes in gene expression in TNF-α-stimulated HUVECs using a cDNA microarray. After TNF-α stimulation several genes were upregulated, such as inhibitor of NF-κB (I-κB), vascular cell adhesion molecule-1 (VCAM-1), and E-selectin, as listed in Table 1.

In contrast, 30 μM EPQB abolished the upregulation of several TNF-α-induced genes (Fig. 1B and Table 1). Correlating with parallel changes in mRNA levels, EPQB significantly suppressed cell adhesion by inhibiting the expression of cell adhesion molecules, such as ICAM1, VCAM1, and E-selectin, at the protein level in a dose-dependent manner (Supplemental Fig. 1; see *Biosci. Biotechnol. Biochem.* Web site). These results suggest that EPQB has an inhibitory effect against TNF-α-induced NF-κB signals.

Table 1. Down-Regulated Genes upon Treatment with EPQB

Gene symbol	Gene name	Ratio#	Ratio*
ICAM1	Intercellular adhesion molecule 1 (CD54), human rhinovirus receptor	1.29	0.53
ICAM2	Intercellular adhesion molecule 2	1.01	0.38
IFNA1	Interferon, alpha 1	0.67	0.58
IL1A	Interleukin 1, alpha	1.98	0.66
IL8	Interleukin 8	1.13	0.65
JUN	V-jun sarcoma virus 17 oncogene homolog (avian)	0.87	0.70
TAK1	Mitogen-activated protein kinase kinase kinase 7 (MAP3K7)	1.11	0.51
NF-κB1	Nuclear factor of kappa light polypeptide gene enhancer in B-cells 1 (p105)	1.23	0.46
NF-κB2	Nuclear factor of kappa light polypeptide gene enhancer in B-cells 2 (p49/p100)	1.41	0.52
I-κBa	Nuclear factor of kappa light polypeptide gene enhancer in B-cells inhibitor, alpha	1.39	0.65
CCL2	Chemokine (C-C motif) ligand 2	1.09	0.72
E-selectin	Selectin E (endothelial adhesion molecule 1)	1.12	0.55
TNFAIP3	Tumor necrosis factor, alpha-induced protein 3	1.10	0.45
VCAM1	Vascular cell adhesion molecule 1	2.01	0.41

Ratio#: [TNF-α stimulated control sample/TNF-α non-stimulated control sample]
Ratio*: [TNF-α stimulated EPQB treatment sample/TNF-α stimulated control sample]

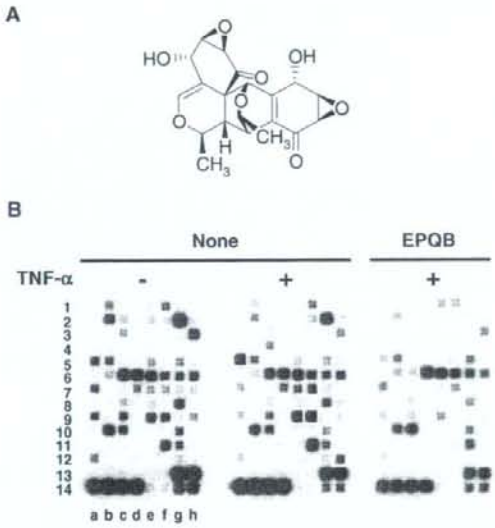

Fig. 1. Changes in TNF-α-Induced Gene Expression in HUVECs under EPQB Treatment.

A, Structure of epoxyquinol B (EPQB). B, cDNA microarray of NF-κB signaling. HUVECs were cultured and treated with and without EPQB for 2 h. After stimulation with and without TNF-α (20 ng/ml) for 1 h, total RNA was extracted. cDNA microarrays were assessed by cDNA GEArray for human NF-κB signaling. The up- and down-regulated genes were a-5, interleukin 8; c-3, interferon α1; c-4, interleukin 1 α; c-6, TAK1; d-7, NF-κB1; e-5, V-jun sarcoma virus 17 oncogene homolog; e-7, NF-κB2; e-9, Chemokine ligand 2; f-2, ICAM2; f-7, I-κBa; f-9, E-selectin; f-11, TNF-α induced protein 3; g-2, ICAM2; and h-12, VCAM1.

EPQB inhibits the nuclear translocation of NF-κB

Because nuclear translocation of NF-κB is vital to TNF-α-induced NF-κB signaling, we investigated the effect of EPQB on NF-κB p65 localization in HeLa cells. In most cells, NF-κB p65 was localized to the cytoplasm without TNF-α stimulation, and in only a fraction of the cells was p65 observed in the nuclei (22.9 ± 3.26% cells). Forty minutes after TNF-α stimulation, NF-κB shuttled into the nuclei in most cells (64.3 ± 3.77% cells), but this translocation was completely blocked by 10 μM EPQB (28.1 ± 2.32% cells).

Moreover, an electrophoretic mobility shift assay using nuclear extract from EPQB-treated cells revealed that TNF-α-stimulated NF-κB binding to its target DNA was inhibited by EPQB in a dose-dependent manner. This inhibition did not occur, however, when EPQB was added to nuclear extract preparations of TNF-α treated cells (Supplemental Fig. 2; see *Biosci. Biotechnol. Biochem.* Web site). These results suggest that EPQB inhibits TNF-α-induced nuclear translocation of NF-κB.

EPQB inhibits TNF-α induced phosphorylation of TAK1 in situ *and the kinase activity of recombinant TAK1-TAB1 protein* in vitro

To characterize the effect of EPQB on TNF-α signaling, we examined TNF-α-induced phosphorylation of TAK1, IKKβ, and I-κB by Western blot. TAK1, IKKβ, and I-κB were dephosphorylated in unstimulated cells, but became significantly phosphorylated after TNF-α stimulation. Yet EPQB inhibited TNF-α-induced TAK1, IKKβ, and I-κB phosphorylation in a dose-dependent manner (Fig. 2A). Because TAK1 is upstream of IKKβ and I-κB, these results suggest that EPQB either inhibits TAK1 directly or acts on proteins that are upstream of TAK1.

TAK1 participates in the TAK1/TAB1/TAB2 complex, which is activated by polyubiquitin chain transfer from RIP to the zinc finger domain of TAB2.[13,14] Hence, we tested the effects of EPQB on TNF-α-induced RIP polyubiquitination by immunoprecipitation assay with anti-RIP antibody. As shown in Fig. 2B, RIP was polyubiquitinated after TNF-α stimulation, and EPQB did not inhibit the polyubiquitination of RIP.

Next we tested *in vitro* TAK1 kinase activity to determine whether EPQB would directly inhibit TAK1. Recombinant TAK1-TAB1 fusion protein phosphor-